

Opinion: Eliminating aircraft soot emissions

Una Trivanovic and Sotiris E. Pratsinis

Particle Technology Laboratory, Department of Mechanical and Process Engineering, ETH Zürich, 8092, Switzerland

Correspondence to: Sotiris E. Pratsinis (sotiris.pratsinis@ptl.mavt.ethz.ch)

1 Abstract

2 Soot from aircraft engines deteriorates air quality around airports and can contribute to climate change primarily
3 by influencing cloud processes and contrail formation. Simultaneously, aircraft engines emit carbon dioxide (CO₂).
4 nitrogen oxides (NO_x) and other pollutants which also negatively affect human health and the environment. While
5 urgent action is needed to reduce all pollutants, strategies to reduce one pollutant may increase another, calling for
6 a need to decrease, for example, the uncertainty associated with soot's contribution to net Radiative Forcing (RF)
7 in order to design targeted policies that minimize the formation and release of all pollutants. Aircraft soot is
8 characterized by rather small median mobility diameters, $d_m = 8 - 60$ nm, and at high thrust, low (< 25%) organic
9 carbon to total carbon (OC/TC) ratios while at low thrust the OC/TC can be quite high (> 75%). Computational
10 models could aid in the design of new aircraft combustors to reduce emissions, but current models struggle to
11 capture the soot d_m , and volume fraction, f_v , measured experimentally. This may be in part due to oversimplification
12 of soot's irregular morphology in models and a still poor understanding of soot inception. Nonetheless, combustor
13 design can significantly reduce soot emissions through extensive oxidation or near-premixed, lean combustion.
14 For example, lean premixed prevaporized combustors significantly reduce emissions at high thrust by allowing
15 injected fuel to fully vaporize before ignition while low temperatures from very lean jet fuel combustion limit the
16 formation of NO_x. Alternative fuels can be used alongside improved combustor technologies to reduce soot
17 emissions. However, current policies and low supply promote the blending of alternative fuels at low ratios (~1%)
18 for all flights, rather than using high ratios (> 30%) in a few flights which could meaningfully reduce soot
19 emissions. Here, existing technologies for reducing such emissions through combustor and fuel design will be
20 reviewed to identify strategies that eliminate them.

21 1. Introduction

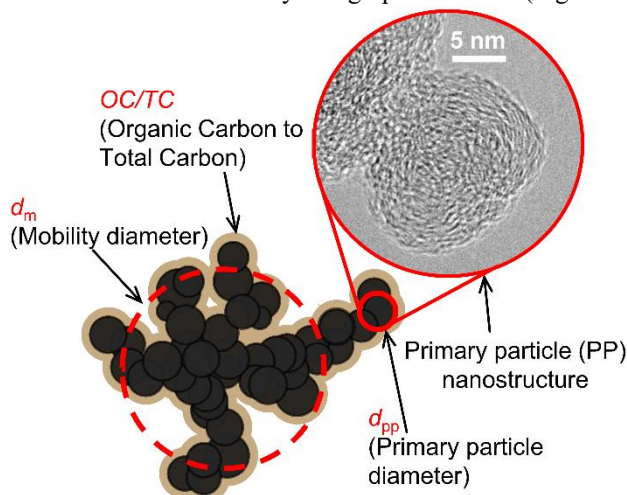
22 Aviation is a growing industry with a significant impact on human health and the environment due to the emission
23 of combustion by-products, including soot aerosols. The latter is one of the most important contributors to climate
24 change (Bond et al., 2013) and a component of air pollution known to cause cancer, cardiovascular and respiratory
25 diseases, and it has been correlated with various other illnesses (Niranjan and Thakur, 2017). For aviation in
26 particular, the adverse health effects of aircraft emissions are partly due to non-volatile particle matter (Delaval et
27 al., 2022) and aircraft soot has similar toxicity to diesel exhaust particles (Bendtsen et al., 2019). Regulations
28 around the world have been limiting soot emissions since the 1970s. The International Civil Aviation Organization
29 (ICAO) until recently limited only the 'smoke number', intended to control visible smoke from aircraft engines
30 which caused dangerous reductions in visibility around airports (George et al., 1972). Modern engines have no
31 visible smoke but still produce invisible nanoparticles (Durdina et al., 2017). In 2020, smoke number was replaced
32 with a limit on the mass concentration of non-volatile Particulate Matter (nvPM) and in 2023 an additional limit
33 was placed on the number concentration of nvPM for all new engines with a rated thrust greater than 26.7 kN
34 (ICAO, 2017). The regulatory term nvPM refers to particles that remain solid when heated to 350 °C. In aircraft
35 emissions, this is primarily soot and concentrations are measured with instruments designed for soot with a low
36 OC/TC ratio (Lobo et al., 2015b) so the terms nvPM and soot will be used interchangeably. Furthermore,
37 regulations on aircraft emissions apply only to turbofan and turbojet engines with rated thrust > 26.7 kN. Volatile
38 particles, lubrication oil particles and secondary organic aerosol may also have important health and climate
39 impacts however, they are not currently regulated and so will not be covered here. Thus, jet engine manufacturers
40 must design new engines to meet the new nvPM standards without exceeding the regulations limiting nitrogen
41 oxides (NO_x), unburned hydrocarbons (UHC) or carbon monoxide (CO) emissions while still maintaining strict
42 safety standards. These regulations are aimed at improving local air quality, so engines are assessed based on a
43 standardized landing and take-off (LTO) cycle most relevant for emissions near the ground.

44 Soot emissions can impact the climate by warming the atmosphere through direct Radiative Forcing (RF)
45 and indirectly by altering cloud processes and decreasing snow albedo (Bond et al., 2013). Aviation is unique in
46 that it emits soot at high altitude with very different atmospheric conditions (e.g., temperature and pressure) from

47 those on the ground. This may influence the formation of contrails (Kärcher, 2018). Lee et al., (2021) estimated
48 the climate forcing contribution of carbon dioxide (CO₂), contrail cirrus, NO_x, soot aerosols, SO₂ aerosols and
49 water vapor from aviation in 2018. By these estimates, contrails account for 57.4 mWm⁻² or 55% of aviation's net
50 radiative forcing but with 95% confidence intervals from 27 – 67% of the net RF illustrating the high uncertainty.
51 The exact RF of contrail cirrus depends on the atmospheric conditions along the flight track and time of day. At
52 night, contrails have an exclusively warming effect while during the day there can be a warming and a cooling
53 effect (Stuber et al., 2006).

54 The estimate of direct RF from soot was relatively low, 0.9 mWm⁻² (Lee et al., 2021). However,
55 inventories of global soot emissions from aircraft can vary by two orders of magnitude (Agarwal et al., 2019).
56 Present inventories are based on the LTO cycle which focuses on landing and take-off at sea-level rather than high-
57 altitude cruise. As these emissions are measured only at ground level for the LTO cycle, the emissions most relevant
58 for climate considerations are only indirectly estimated (Stettler et al., 2013). Estimates of emissions inventories
59 must convert values measured at the ground to account for the drastically different atmospheric conditions at cruise
60 (Teoh et al., 2024). In addition, the LTO cycle does not exactly match the real time at each thrust for example, the
61 LTO cycle assumes idle/taxi is 7% but real aircraft use between 3 – 17% thrust for these conditions (Masiol and
62 Harrison, 2014). Estimates of the RF of soot are from climate models which may underestimate the contribution
63 of soot (Kelesidis et al., 2022). While CO₂ remains in the atmosphere for 100 years or more, soot and contrails
64 have short atmospheric lifetimes on the order of a week (Bond et al., 2013) or hours (Bock and Burkhardt, 2016),
65 respectively, so their global warming potential is most important in the short term. This presents an opportunity to
66 make immediate reductions in global warming and 'buying time' for the implementation of technologies to lower
67 CO₂ emissions (Montzka et al., 2011). This may be important for the aviation industry which in 2022, adopted an
68 ambitious goal of net-zero carbon emissions by 2050.

69 These uncertainties highlight the importance of further research to better quantify the role of soot in both
70 contrail formation (Marcolli et al., 2021) and direct radiative forcing (Kelesidis et al., 2022). In particular, the role
71 of soot in contrail formation is still unclear and there is high uncertainty in the RF of aviation aerosol-cloud
72 interactions (i.e. indirect RF) and therefore no best estimate is given by Lee et al. (2021). Such uncertainties make
73 it difficult to accurately assess priorities in emission reductions as there are often trade-offs between emissions.
74 For example, there is a well-established trade-off between soot and NO_x in diesel engines (Kim et al., 2009) which
75 has also been observed in aircraft combustors (Harper et al., 2022). Similarly, contrail formation can be avoided
76 by diverting flights to airspace with unfavorable conditions for contrail formation (e.g. warmer temperatures) but
77 may result in higher fuel consumption and, thus, CO₂ emissions (Teoh et al., 2020). The large uncertainty
78 associated with the contribution of soot to climate change is in part due to the oversimplification of soot
79 morphology and composition in climate models which typically assume soot to be coated spheres (Kelesidis et al.,
80 2022). In reality, soot is an agglomerate composed of polydisperse primary particles (PP), illustrated in Figure 1,
81 with a nanostructure of layered graphene sheets (Fig. 1: inset).



82
83 **Figure 1: A schematic of a soot nanoparticle highlighting commonly quantified properties which are relevant for**
84 **assessing the health and climate impact of such particles including the mobility diameter, d_m (broken line), primary**
85 **particle diameter, d_{pp} (solid line) and Organic Carbon (brown shaded area) to Total Carbon ratio, OC/TC. The inset**
86 **shows a high-resolution transmission electron micrograph (HRTEM) of a soot primary particle, from enclosed spray**
87 **combustion of jet fuel produced at an equivalence ratio of 1.25 (Trivanovic et al., 2022), where the individual graphene**
88 **layers can be seen. Volatile compounds that may be adsorbed on the surface usually evaporate under the vacuum of the**
89 **microscope so cannot be visualized easily with HRTEM.**

90 The relative amounts of Organic Carbon (OC) or Elemental Carbon (EC) compared to the Total Carbon
91 (TC) is typically used to quantify the chemical composition of the particles. The OC is defined by the ICAO as
92 "...carbon volatilized in Helium while heating a quartz fiber filter sample to 870 °C during thermal optical
93 transmittance analysis including char formed during pyrolysis of some materials". Conversely, EC is "...light
94 absorbing carbon that is not removed from a filter sample heated to 870 °C in an inert atmosphere during thermal
95 optical transmittance analysis, excluding char" (ICAO, 2017). The OC/EC ratio is important for source
96 apportionment of ambient aerosols (Ramadan et al., 2000), attempting to understand the health effects of soot
97 (Kelly and Fussell, 2012) and for determining the light absorption of soot (Kelesidis et al., 2021). However, the
98 split between EC and OC is method-dependent (Cavalli et al., 2010) rather than a discrete property. The size of
99 irregular agglomerates such as soot is quantified by equivalent diameters for example, electrical mobility diameter,
100 d_m (Fig. 1: broken line), aerodynamic diameter or projected area equivalent diameter where the type of equivalent
101 diameter depends on the measuring principle. Such agglomerate diameters can be several times larger than the
102 mass-equivalent diameter typically calculated by models (Eggersdorfer and Pratsinis, 2014). Using a realistic soot
103 morphology rather than equivalent spheres in climate models increases the estimated direct RF by 20% on average
104 revealing large direct RF = 3 – 5 W/m² in hot spot earth regions, in line with field observations (Kelesidis et al.,
105 2022).

106 Furthermore, limited access to real jet engines has made it difficult to assess the efficiency of soot to act
107 as ice condensation nuclei (ICN) and thus to enhance contrail formation although recently there have been efforts
108 to assess the ICN activity of soot from modern in-use commercial engines (Testa et al., 2024). To date, experiments
109 on the ICN activity of soot have been done primarily using commercial carbon blacks or miniCAST soot generated
110 by burning hydrocarbon gases (Gao et al., 2022). MiniCAST particles tend to have much larger d_m (> 100 nm)
111 than that produced by real aircraft (< 100 nm) if the organic carbon to total carbon ratio (OC/TC) is sufficiently
112 small (Durdina et al., 2016). Recently, enclosed spray combustion of jet A1 fuel has been shown to be a promising
113 laboratory surrogate for aircraft soot produced at high thrust (i.e. cruise) with sufficiently small d_m and OC/TC
114 (Trivanovic et al., 2022). This is important for the calibration of optical instruments which may be sensitive to the
115 OC/TC ratio in addition to particle morphology (Durdina et al., 2016).

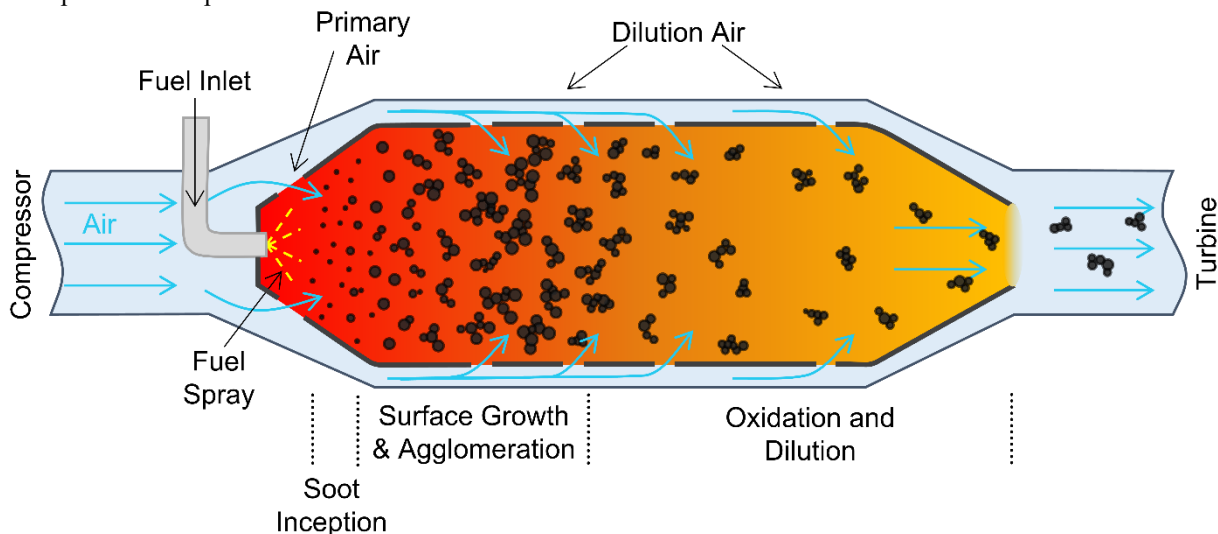
116 Technology for battery-electric or hydrogen-powered planes will not be available in the short-to-medium
117 term for long-haul flights (Schäfer et al., 2019). Significant investment in airport infrastructure would be needed
118 to accommodate such changes in technology (Agnolucci et al., 2013). Emissions from aviation need to be
119 addressed urgently to meet climate goals and prevent further health degradation and mortality from air pollution.
120 However, aircraft engines have many competing demands including continued reduction of gaseous emissions,
121 CO₂ net-zero goals, safety requirements and regulations on noise. Thus, a firm understanding of the environmental
122 and health impacts of soot as well as a fundamental understanding of its formation and growth in aircraft engines
123 is essential for weighing the costs and benefits of mitigation strategies. As regulations apply only to turbofan and
124 turbojet engines with rated thrusts > 26.7 kN, most scientific research has been conducted on engines in this
125 category and will also be the category discussed in this paper. However, it is worth noting that small business jets
126 with thrusts < 26.7 kN may produce more nvPM emissions than large aircraft such as the Boeing 737 which do
127 fall under the ICAO regulations and need further research for accurate emissions inventories (Durdina et al., 2019).
128 In addition, leaded aviation gasoline (Avgas) is responsible for lead-containing aerosols internally or externally
129 mixed with soot. While the European Union (EU) voted to ban leaded Avgas used in small piston-engine aircraft
130 in 2022, most other countries still allow its use and it is now considered one of few major sources of ambient lead
131 in the US (National Academies of Sciences Engineering and Medicine, 2021). Possible mechanisms for the
132 formation and dynamics of soot from regulated jet engines will be discussed here. Then, strategies already in use
133 or under development for the elimination of jet engine soot emissions will be reviewed.

134 2. Formation and dynamics of aircraft soot

135 Although aircraft combustor design can vary significantly, the soot produced by aircrafts have some morphological
136 and compositional differences from other sources such as diesel engines. Aircrafts tend to produce soot with
137 median d_m in the range of 8 (Durdina et al., 2021) to 60 nm (Abegglen et al., 2015). Such small d_m are associated
138 with greater lung deposition efficiency (Rissler et al., 2012) and translocate from the lungs to other organs more
139 effectively than particles with d_m > 100 nm (Cassee et al., 2013). The OC/TC tends to be quite low (< 25%)
140 (Marhaba et al., 2019) when the aircraft operates at high thrust (> 50%) while the reverse is true at low thrust. The
141 OC/TC influences the optical properties of soot and thus its RF (Kelesidis et al., 2021) and will impact the output
142 of optical instruments used to measure aircraft emissions (Durdina et al., 2016). Aircraft soot has PP diameters,
143 d_{pp} (Fig. 1: solid line), from approximately 5 (Liati et al., 2019) up to 24 nm with lower thrusts tending to produce
144 smaller d_{pp} (Liati et al., 2014) which influences soot reactivity (Messerer et al., 2006) and optical properties
145 (Kelesidis et al., 2020). These same properties are also influenced by PP nanostructure which is related to their

146 maturity (Baldelli et al., 2020). Aircraft tend to produce rather disordered soot with a turbostratic structure with
 147 more defects on its surface than the bulk (Parent et al., 2016). The conditions under which soot forms determine
 148 its final morphology and composition and *vice versa* (Vander Wal et al., 2010).

149 Figure 2 depicts the cross-section of a single annular aircraft combustor (SAC), one of the common
 150 combustor designs in modern engines. The combustor is typically an annular tube that receives high pressure air
 151 from the compressor, adds energy to the system through combustion and uses it to drive the turbine. Liquid jet fuel
 152 is injected at one end of the SAC, typically with a swirling mechanism to atomize the fuel, promoting evaporation.
 153 However, perfect mixing is not achieved. So locally fuel-rich pockets allow for soot formation even if the global
 154 mixture is fuel-lean. Where the fuel is injected, there is significant recirculation allowing soot to grow in these
 155 fuel-rich pockets (Gkantonas et al., 2020). When there is insufficient oxygen for complete conversion to carbon
 156 dioxide, fuels decompose into radicals and intermediate species, such as acetylene which then grow into small
 157 aromatics (Wang, 2011). These aromatic compounds eventually evolve into polycyclic aromatic hydrocarbons
 158 (PAHs) which are the key gaseous precursors to soot (Frenklach, 2002). The presence of these soot precursors has
 159 been confirmed experimentally with atomic force microscopy (Commodo et al., 2019). With respect to aviation,
 160 experimental studies have shown a correlation between jet fuel aromatic content, sooting tendency (Yang et al.,
 161 2007) and nvPM emissions (Brem et al., 2015). So, fuel composition plays a key role in the formation of soot and
 162 thus provides one possible route for its elimination as discussed in detail in the next section.



163
 164 **Figure 2: A simplified schematic of an aircraft single annular combustor (SAC) adapted from (Foust et al., 2012) with a**
 165 **qualitative depiction of the soot dynamics from soot inception to surface growth & agglomeration and then oxidation**
 166 **before being vented to the turbine and eventually the exhaust.**

167 Although the exact mechanisms of soot nucleation (i.e. the transition from the gas to solid phase) are still an
 168 area of active research (Carbone et al., 2023), the dynamics of soot inception (Sharma et al., 2021) and growth
 169 from nascent to mature soot (Kelesidis et al., 2017b) leading to its final structure are becoming better understood.
 170 Nascent soot particles are as small as $d_m \sim 2$ nm (Camacho et al., 2015), amorphous (Commodo et al., 2017) and
 171 liquid-like (Kholghy et al., 2013) with a carbon to hydrogen (C/H) ratio < 2 (Schulz et al., 2019). As they age,
 172 nascent soot carbonizes (loses hydrogen) and solidifies (Dobbins, 2002). Soot then simultaneously undergoes
 173 surface growth and agglomeration (Kelesidis et al., 2017a). Surface growth of soot is well described by the
 174 hydrogen-abstraction carbon-addition (HACA) mechanism (Frenklach, 2002) although other pathways have also
 175 been proposed (Wang, 2011). During the first few milliseconds of particle growth, surface growth precursors are
 176 depleted then agglomeration takes over as the primary growth mechanism and d_m increases markedly while d_{pp}
 177 stays approximately constant (Kelesidis et al., 2017a). In the free molecular regime, particles grow into large
 178 agglomerates through ballistic cluster-cluster coagulation while in the continuum regime this becomes diffusion-
 179 limited cluster agglomeration. Particles which coagulate in the free molecular regime have a slightly more compact
 180 structure than those in the continuum regime as shown by their asymptotic mass fractal dimensions of 1.91 and
 181 1.78, respectively (Goudeli et al., 2015).

182 This soot growth sequence has been observed and quantified for soot formation in premixed flames, diesel
 183 engines, miniCAST soot generator (Kelesidis et al., 2017b) and even for enclosed spray combustion of Jet A1 fuel
 184 resulting in aircraft-like soot (Trivanovic et al., 2023). After primary air injection for the initial combustion,
 185 dilution air is added at various locations along the combustor length. This oxidizes a sizable portion of the soot
 186 which was initially created. Transmission Electron Microscopy (TEM) has shown that aircraft soot is significantly
 187 oxidized and the small d_m may be in part due to fragmentation of larger agglomerates after extensive oxidation

188 (Vander Wal et al., 2014). So, in the early stages of the combustor the number and size of soot is likely larger than
189 what is eventually emitted. The final morphology of the particles, including the d_{pp} , d_m and number of PPs per
190 agglomerate, n_p , depends on the initial volume fraction, residence time, temperature and pressure (Kelesidis et al.,
191 2023a).

192 While conditions can vary significantly depending on the engine, soot in an aircraft combustor
193 experiences both high temperature and pressure. In addition, pressures are increased at high thrust which has been
194 correlated with increased soot concentration and size (Chu et al., 2023). Higher pressures improve the efficiency
195 of engines and so as engine materials have been improved to withstand higher pressures, the pressure ratios in
196 engines have also increased. So, soot may begin growing in the free molecular regime but enters the transition
197 regime as it grows, in particular at high thrust, when pressures are the highest and soot particles tend to grow to
198 the largest sizes. This is in line with mass-mobility measurements of aircraft soot which shows an increase in the
199 mass-mobility exponent, D_{fm} , from 1.86 ± 0.37 to 2.79 ± 0.07 as thrust increases from 7 to 118%, respectively
200 (Abegglen et al., 2015). However, mass-mobility measurements are not part of the regulatory framework for
201 aircraft nvPM.

202 Low thrusts lead to the longest soot residence time in the combustor but tend to produce the smallest
203 particles both in terms of d_m and d_{pp} which can be attributed to the smaller amount of fuel resulting in a lower
204 volume fraction of nascent soot (i.e. less nucleation) and allowing for a longer residence time in oxygen rich zones
205 which oxidizes the soot reducing both the number and size of particles (Durdina et al., 2014). At the same time,
206 the OC/TC increases at low thrust which could be attributed to poorer combustion efficiency at these conditions.
207 At high thrust the residence time is short but initial number concentrations are higher due to high fuel flow. The
208 time in oxidating zones is reduced also, resulting in a larger number concentration, d_{pp} (Liati et al., 2014) and d_m
209 (Abegglen et al., 2015). Simulations of aircraft combustors have shown that soot forms intermittently in locally
210 rich regions of the flame and, due to recirculation, soot spends 4 – 5 times longer in the combustor than the fluid
211 time scales (Chong et al., 2018b). The high-temperature residence time of soot in a combustor can only be
212 estimated from simulations that account for the geometry, fluid flow rates, temperature and pressure in a given
213 combustor.

214 Modeling soot emissions accurately remains a challenge (Chong et al., 2018a) because soot formation in
215 combustors is intermittent. So, simulations must take place over a large time frame to achieve a statistically
216 representative time-averaged result (Franzelli et al., 2023). Furthermore, the transport and chemistry of soot must
217 be solved simultaneously in order to capture the real volume fraction, f_v , and particle size distributions (PSD)
218 (Gkantonas et al., 2020). The most detailed simulations to date have utilized laboratory combustors such as the
219 Cambridge Rich Quench Lean (RQL) burner (Gkantonas et al., 2020). These laboratory burners are optically
220 accessible for laser diagnostics allowing for a detailed comparison to the evolution of soot f_v and PSD. However,
221 the laboratory burners use ethylene, a gas, instead of liquid jet fuel and pressures are up to 5 bar (Chong et al.,
222 2018a). Modern aircraft engines may have pressures up to an order of magnitude higher than this at certain
223 conditions (Nguyen et al., 2019). Nonetheless, such simulations can give insight into the formation and growth of
224 soot in aircraft combustors capturing some of the trends observed experimentally. Specifically, simulations show
225 that soot forms near the shear layers between the fuel and oxidizer streams and then enters an inner recirculation
226 zone where it grows further (Gkantonas et al., 2020). Fuel rich pockets can also break off from the main jet and
227 become entrained in the recirculation zone driving the intermittent soot growth within the combustor (Chong et
228 al., 2018a). Soot was shown to grow by both acetylene-based surface growth (e.g., HACA) and condensation via
229 aromatics (Gkantonas et al., 2020). Simultaneously, significant oxidation reduces the particle size and can induce
230 fragmentation increasing the number concentration (Gkantonas et al., 2020) which is supported by experimental
231 data (Vander Wal et al., 2014). Introduction of dilution air part way through the burner oxidizes soot in the lean
232 combustion zone as well as lowers the rate of soot formation near the nozzle (Chong et al., 2018a). Higher pressures
233 in the model combustor result in larger soot f_v , a trend which was captured by simulations but the total f_v for the
234 high pressure condition was underpredicted by a factor of 4 (Chong et al., 2018a). Therefore, simulations can give
235 insight into the formation of soot in aircraft combustors but significant improvements are needed to have truly
236 predictive models which can aid in combustor design (Franzelli et al., 2023). It is worth noting that these
237 simulations focus on capturing the number and mass emissions from combustors, but do not seem to account for
238 the realistic morphology of soot particles which are highly irregular agglomerates rather than spheres. The
239 assumption that soot is spherical rather than an agglomerate with polydisperse primary particles can significantly
240 change the resulting estimate of soot d_m , number and, most importantly, f_v (Kelesidis and Goudeli, 2021).
241 Therefore, it is not realistic to predict soot formation without properly accounting for its shape (Bouaniche et al.,
242 2020). For example, models overpredict soot volume fraction by up to 3 times when particles are assumed to be
243 spherical (Kelesidis and Pratsinis, 2021). Such realistic descriptions have, for example, been used quite effectively
244 to describe black carbon (BC) formation and growth from a variety of combustion sources and even facilitate

245 monitoring of BC emissions by aerosol (e.g., particle mobility and mass analyzers), laser (e.g., light extinction)
246 diagnostics and fire detectors by accounting for BC morphology and limiting the current uncertainty regarding BC
247 mass and particle size (Kelesidis et al., 2020). In addition, by capitalizing on the accurate description of the high
248 temperature residence time during enclosed combustion synthesis of nanomaterials and the latest advances in soot
249 structure and composition, more than 99% of the emitted soot mass and concentration from enclosed jet fuel
250 combustion was removed (Kelesidis et al., 2023b).

251 3. Means for the elimination of aircraft soot

252 3.1 Sustainable aviation fuels

253 Alternative aviation fuels include any fuels aside from kerosene-based jet fuels and Avgas. This includes, for
254 example, hydrogen, ammonia and jet fuels made without fossil fuels. Sustainable Aviation fuels (SAF) are non-
255 fossil jet fuels that are attractive due to their potential to act as a drop-in solution for reducing CO₂ emissions as
256 these fuels can be used directly in existing engines. The ICAO specifies fuels must be “completely interchangeable
257 and compatible with conventional jet fuel” in order to prevent the safety risks of mishandling and high costs of
258 additional infrastructure (ICAO, 2018). Alternative jet fuels can be considered ‘drop-in’ when they do not require
259 new fuel systems, distribution networks or new aircraft (ICAO, 2018). Sustainable Aviation Fuels (SAF) are
260 mainly produced from biological feedstocks (e.g. soybeans, sugarcane, biomass, etc.) (Staples et al., 2018). These
261 are converted into liquid hydrocarbon fuels through processes such as Hydroprocessed Esters and Fatty Acids
262 (HEFA), Fischer-Tropsch (F-T) or Alcohol-to-Jet (ATJ) to name a few (Brooks et al., 2016). Similarly, e-fuels use
263 CO₂ capture and sustainable energy sources such as solar to produce synthetic jet fuels (Schäppi et al., 2022).
264 Currently, SAF are only certified for use when blended with conventional jet fuel although efforts are being made
265 to certify 100% SAF in the future. Flights powered with 100% SAF have already been performed for research
266 purposes (Märkl et al., 2024). The CO₂ reduction from such fuels comes primarily from the synthetic or biological
267 CO₂ captured during the production process. Actual CO₂ released from the engine remains about the same as
268 conventional jet fuel. So, a Life Cycle Analysis (LCA) is needed to account for the so-called Well-to-Wake
269 emissions (Han et al., 2013). The total reduction in Green House Gas (GHG) emissions will depend on both the
270 GHG emissions associated with production of the petroleum based jet fuel as well as the net GHG emissions from
271 growing, transporting and burning the SAF fuels. The ICAO, under the Carbon Offsetting and Reduction Scheme
272 for International Aviation (CORSIA), certifies alternative fuels as SAF based on a standardized LCA. While the
273 exact reduction in GHGs will change as technologies evolve, an LCA of the best case scenarios show up to a 68%
274 reduction in CO₂ emissions if SAFs account for > 85% of all aviation fuels (Staples et al., 2018).

275 In addition to reducing net-CO₂ emissions, SAFs also have the potential to reduce soot emissions and thus
276 the health impact and non-CO₂ radiative forcing of aircraft emissions which is typically excluded from LCA
277 analysis (Staples et al., 2018). These fuels tend to have a lower aromatic content than fossil fuels which has been
278 correlated to the number of particles emitted by an aircraft (Brem et al., 2015). As discussed previously, aromatic
279 species are key precursors to soot formation and thus a decrease in fuel aromatics may reduce the rate of soot
280 nucleation. The hydrogen-to-carbon ratio (H/C) of the fuel has been shown to have an even greater anti-correlation
281 with aircraft soot emissions than fuel aromatic content (Brem et al., 2015). While H/C has long been associated
282 with the sooting tendency of a fuel (Yang et al., 2007), the mechanism for this is less clear as it is difficult to
283 separate from effects such as lower flame temperatures (Xue et al., 2019). Blends of a HEFA-based SAF with Jet
284 A1 up to 50% (the current upper limit for a SAF blend) showed a ~35% reduction in number based nvPM and
285 ~60% reduction in mass based nvPM (Lobo et al., 2015a). These reductions correlated best with the H/C content
286 of the blends. In fact, the geometric mean d_m has been shown to drop nearly linearly as H/C increases while
287 decreases in nvPM number were not as steep suggesting that the decrease observed in nvPM mass is strongly
288 influenced by the smaller particle sizes for HEFA-based fuels (Durand et al., 2021). Similar trends were observed
289 for a range of different SAF types including HEFA, Alcohol-to-Jet (ATJ) and a Catalytic Hydrothermal Conversion
290 Jet (CHCJ) fuel showing that the dependence on H/C is not dependent on the fuel production method (Harper et
291 al., 2022). The size distributions of the soot produced shifted to smaller mobility diameters from $d_m = 49$ to 22.5
292 nm and narrowed the distribution from a geometric standard deviation, $\sigma_g = 1.99$ to 1.58 with pure Jet A1 and a
293 50% blend, respectively (Lobo et al., 2015a). With pure Jet A1, the σ_g approaches that of the self-preserving limit
294 for agglomerates coagulating in the free-molecular regime (Goudeli et al., 2015) while the σ_g produced with the
295 SAF blends are significantly smaller. This could be due to the decreased number concentration from extended
296 surface growth and less agglomeration. As the aromatic content and H/C of conventional jet fuels varies, the actual
297 reductions achieved with SAF blends will depend on composition of the conventional jet fuel in the blend,
298 particularly when the SAF blending ratio is low. Currently, alternative fuels are designed primarily with the goals
299 of reducing life-cycle CO₂ emissions and matching the properties of conventional jet fuels. However, there is an

300 opportunity to also optimize jet fuel composition for minimum soot emissions. Schripp et al., (2021) showed that
301 different SAF could be blended to obtain a desired H/C, while maintaining regulatory specifications for jet fuels.
302 Soot emissions of these fuels were first tested in a laboratory flame, then the optimal mixture was used in a real
303 jet engine to confirm the trends seen in the laboratory resulting in emission reductions of particle mass and number
304 by 29 and 37%, respectively, when using a 38% SAF blend with Jet A1 (Schripp et al., 2021). However, if a SAF
305 blend is designed with higher aromatic content and lower H/C than a conventional fuel, soot emissions could even
306 increase (Schripp et al., 2019). Laboratory tests are essential for speeding up the design of alternative fuels since
307 real jet engines are inaccessible to many researchers and too costly to operate for initial screening tests. A
308 standardized flame for assessing the sooting properties of jet fuels would assist in the development of alternative
309 fuels however, there is currently no standardized method for such experiments. Enclosed spray combustion is a
310 promising unit for such in lab approaches (Trivanovic et al., 2022).

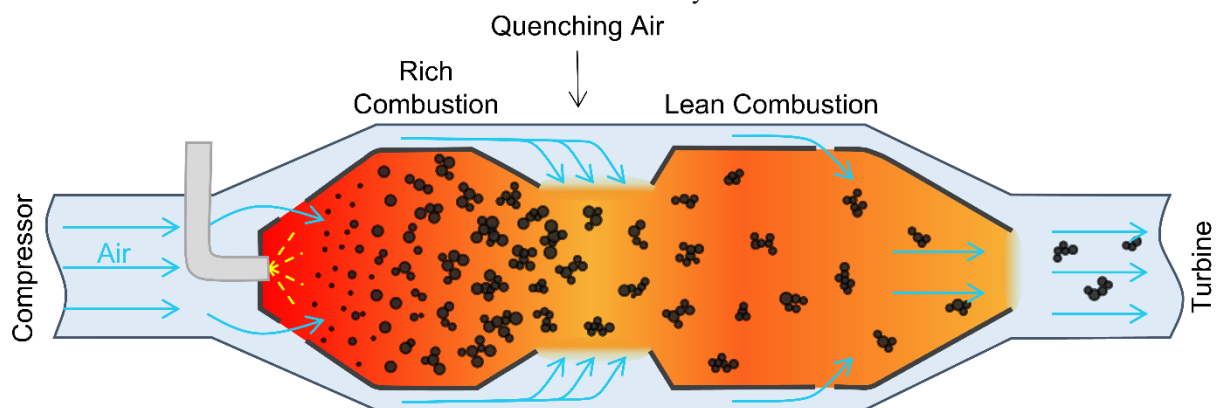
311 Several publications have shown that the benefits of a SAF blend are thrust-dependent. For example, a
312 32% blend of HEFA-synthetic paraffinic kerosene and Jet A1 at idle operation showed a 60 and 70% reduction in
313 number- and mass-based nvPM, respectively (Durdina et al., 2021). The same blend at 65% thrust resulted in only
314 a 12% reduction in number-based nvPM and at take-off the reduction was only 7%. In this case, the use of such
315 SAF blends may improve local air quality by reducing emissions in the vicinity of airports but may not make a
316 significant impact on cruise conditions which are most concerning for climate change. It is worth noting that the
317 majority of studies on aircraft soot emissions are done at ground level which has significantly different atmospheric
318 conditions than cruise in the upper atmosphere. Ideally, cruise emissions should be measured behind an aircraft in-
319 flight, but this is rarely done due to the cost and logistical challenges. One of the few in-flight studies comparing
320 conventional jet fuel to a 50% HEFA blend showed a 50 and 70% reduction in particle number and mass emissions,
321 respectively, behind an aircraft with a medium thrust setting of ~ 50% (Moore et al., 2017). At the high thrust
322 setting, the particle number reduction was only 25% (Moore et al., 2017), supporting the trend observed on the
323 ground. The wide range of values listed here highlights the need for more studies both at the ground level and in-
324 flight.

325 Currently, SAF must be blended with conventional jet fuel (up to 50%) for safety reasons although 100%
326 blends may be allowed by 2030. In practice, supply issues keep the use of SAF low accounting for an estimated
327 0.1 – 0.15% of global jet fuel use in 2022 despite a tripling in the supply of SAF from 2021 to 2022. If the SAF
328 supply is limited and individual flights only have a very small fraction of SAF in the fuel, there will likely be no
329 effect on the soot emissions (Lobo et al., 2015a). So, while alternative fuels could provide a short-term solution to
330 reducing aircraft emissions, the speed at which this is adopted is still limited. Targeted use of the limited SAF
331 supply could be used in the short term to maximize the benefits of such fuels while supply is limited. For example,
332 contrails with the greatest warming effect are commonly at dusk during the winter (Teoh et al., 2022a) so fueling
333 flights at such times with high SAF blends could have the biggest benefit. One analysis found that compared to a
334 1% SAF blend for all transatlantic flights, fueling the 2% of flights producing the highest RF with a 50% SAF
335 blend could take the total RF reduction from 0.6% up to 6% (Teoh et al., 2022b). The European Commission and
336 the US have implemented policies to mandate the annual uptake of SAF which may prohibit the targeted use of
337 SAF. For example, starting in 2025 it will be required that “all aviation fuel supplied to aircraft operators at
338 (European) Union airports contains a minimum share of SAF” (European Commission, 2021). Further press
339 releases confirm that “this means that every flight leaving the larger EU airports, will carry a minimum amount of
340 SAF” (Fit for 55 and ReFuelEU Aviation). Some airlines have made similar pledges for example, Air France KLM
341 promises they “will add a percentage (0.5% to 1%) of SAF on all flights departing from France and the
342 Netherlands” (Air France KLM Sustainable Aviation Fuel). Thus, while the supply of SAF is limited, it will be
343 used in more aircraft at lower blending ratios missing an opportunity to reduce soot emissions. Intelligent changes
344 to policy on the use of alternative fuels could thus reduce the net-RF of aviation without needing to increase the
345 supply of SAF.

346 3.2 Aircraft Combustor Design & Operation

347 The limitations of alternative jet fuels highlight the continued need for improved and novel engine technologies
348 which could be used also with alternative fuels to minimize the total impact of aviation on the environment. Here,
349 only combustion engines will be considered as electric aircrafts are estimated to account for only a quarter of all
350 passenger-miles in 2050 (Prabhakar et al., 2022). Furthermore, some in-development technologies, such as open
351 rotor engines, promise significant reductions in fuel consumption (Khalid et al., 2013) and soot emissions but are
352 not discussed here as they are not linked to the actual formation of soot. Since nvPM regulations only recently
353 came into effect, most aircraft combustors are designed primarily to lower NO_x, but some designs can also reduce
354 soot. Alternative fuels have not been shown to reduce NO_x emissions compared to conventional jet fuel (Moore
355 et al., 2017). Combustor designs must balance limits for all regulated gas and particulate emissions, fuel efficiency,

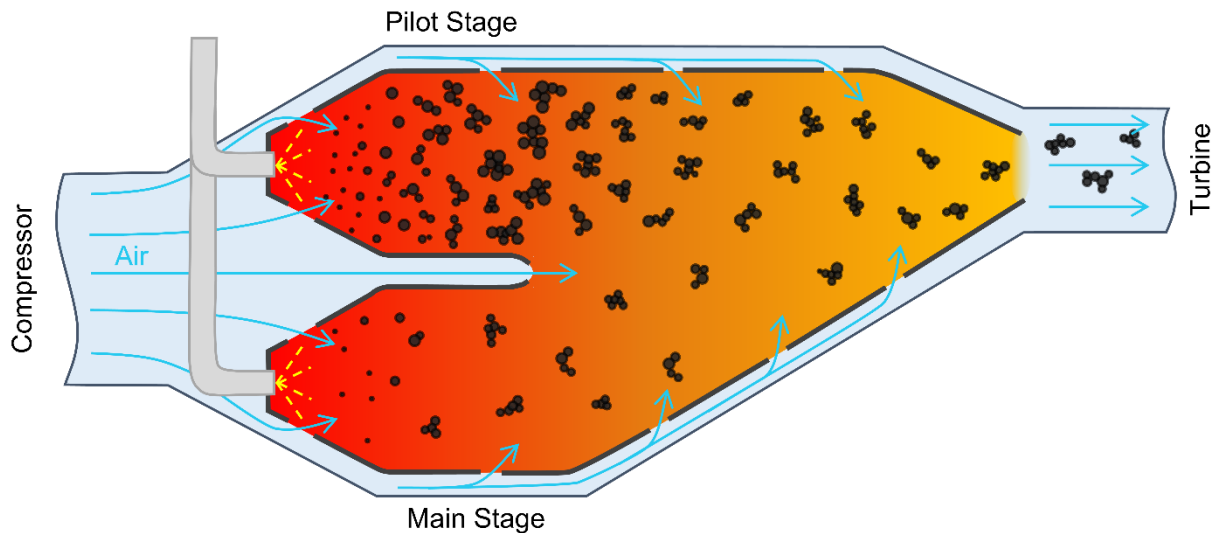
356 safety and cost. Rich Quench Lean (RQL) combustors have been used by the aviation industry since at least the
 357 1980s to reduce NO_x emissions while maintaining sufficient combustion stability (Novic et al., 1983). Today, they
 358 are the most common type of combustor listed in the ICAO emissions database (ICAO Aircraft Engine Emissions
 359 Databank, 2023). Briefly, RQL combustors have three zones, depicted in Figure 3. First, there is a fuel-rich zone
 360 that allows for more stable combustion which is important for the safety of the aircraft. Rich conditions have lower
 361 combustion efficiency and promote the formation of soot, UHCs, and CO. In the quenching zone, a large volume
 362 of cool air is injected to provide oxygen for completing the conversion of UHCs and CO to CO₂ while lowering
 363 the temperature to minimize NO_x formation. The air flow for the rich combustion stage and quenching zone are
 364 controlled separately and further dilution air may be added before the gases are sent to the turbine. Although the
 365 mixing and residence times in RQL combustors were originally optimized for reducing NO_x (Rizk and Mongia,
 366 1990) proper design and operation can also reduce soot emissions through oxidation during the lean burn stage. In
 367 fact, it was shown in a laboratory setting that a judicious injection of fresh oxygen in a manner similar to RQL
 368 combustors can promote oxidation of soot removing up to 99.6% of the initial soot volume fraction from jet fuel
 369 combustion (Kelesidis et al., 2023b). Such results can be scale up by matching the high temperature residence time
 370 as has been shown with scale-up of flame synthesis of nanoparticles from mg to kg per hour (Kelesidis and
 371 Pratsinis, 2021). When quenching air is introduced farther downstream in the combustor, soot has more time to
 372 form and grow. Hence, oxidation is less effective. Earlier injection of air with sufficient turbulent mixing has the
 373 opposite effect, minimizing soot emissions (El Helou et al., 2021). However, if quenching air is injected too early
 374 this could increase NO_x emissions or reduce combustion stability.



375
 376 **Figure 3: A simplified schematic of a Rich Lean Quench (RQL) aircraft combustor adapted from (Rizk and Mongia,**
 377 **1990) where there is first a fuel rich combustion zone, followed by a large flow of quenching air to lower the temperature**
 378 **and dilute to a globally lean combustion zone. The dynamics of soot are qualitatively depicted from inception to surface**
 379 **growth, agglomeration and oxidation.**

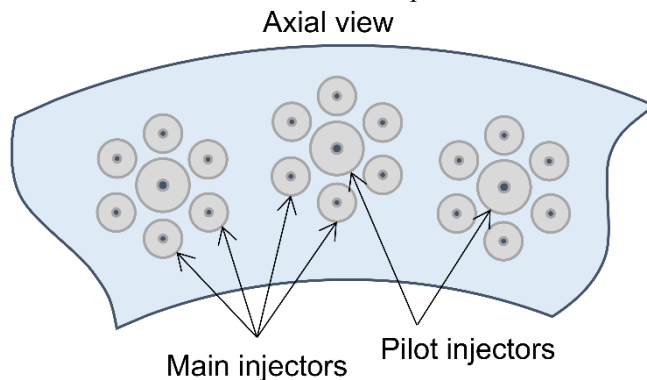
380 In 1995, the first Double Annular Combustor (DAC) was used commercially. This combustor design has
 381 two stages as the name implies, depicted in Figure 4. At low thrust (e.g., idle) only the pilot stage is used with a
 382 low air to fuel ratio and low flowrate to ensure good ignition and to reduce CO and UHC emissions. When
 383 sufficiently high thrust is achieved, both the pilot and main stage are ignited with a high air to fuel ratio (lean burn)
 384 and high flowrates (Boies et al., 2015). This had the desired effect of reducing the NO_x emissions over the LTO
 385 cycle by ~30% compared to a single annular combustor on the same engine (Mongia, 2007). Soot emissions from
 386 a DAC equipped engine vary significantly with thrust. At low thrust, when only the pilot stage is ignited, soot
 387 emissions are high, and increase with increasing thrust in both number and mobility diameter (Boies et al., 2015).
 388 When both stages are ignited at thrust ~25%, the soot concentration and size drops significantly (Boies et al.,
 389 2015). Similarly, a DAC using only the pilot stage showed an increased mass concentration of organic particulate
 390 matter compared to when both stages were used (Lobo et al., 2015b). The morphology of soot produced in both
 391 stages is in the range observed in other combustors.

392 As demonstrated by the low emissions of DAC when operated in the lean combustion mode, lean burn
 393 engines have the potential for extremely low emissions if the combustion stability issues can be overcome. In fact,
 394 lean combustion technologies typically produce an order of magnitude less soot than an RQL combustor (Liu et
 395 al., 2017). Lean burn combustors were first developed for stationary gas turbines used for energy generation where
 396 safety requirements are less strict and are now being transferred to aviation as technology improves. Such
 397 technologies include Lean Direct Injection (LDI) or the Multipoint Lean Direct Injection concept (MLDI) (Liu et
 398 al., 2017). Direct injection is used to reduce the risk of autoignition that comes with premixed combustion. The
 399 use of multiple injectors, depicted in Figure 5, along with intense mixing creates conditions similar to lean,
 400 premixed combustion. In an LDI combustor a central pilot injector is surrounded by multiple main fuel injectors



401
 402 **Figure 4: Simplified schematic of a Double Annular Combustor (DAC) adapted from (Foust et al., 2012) and a**
 403 **qualitative depiction of the dynamics of soot surface growth, agglomeration and oxidation within the combustor.**

404 with little to no dilution added after the initial air supply near the fuel injectors. The MLDI concept is similar to
 405 the LDI combustor with an altered injector layout. Globally lean combustion with good mixing is unfavorable for
 406 soot production as there are few locally fuel-rich areas. At the same time, low temperatures from the lean burn
 407 reduce NO_x emissions significantly (Liu et al., 2017). Regulatory measurements of nvPM emissions from an LDI
 408 combustor show nvPM mass and number emission levels on par with RQL combustors with similar rated thrusts
 409 (ICAO Aircraft Engine Emissions Databank, 2023). To the best of our knowledge, no studies have characterized
 410 the size, morphology or chemical composition of soot from an LDI equipped engine. The limited data for such
 411 combustors makes the real emissions performance of such an engine difficult to assess.

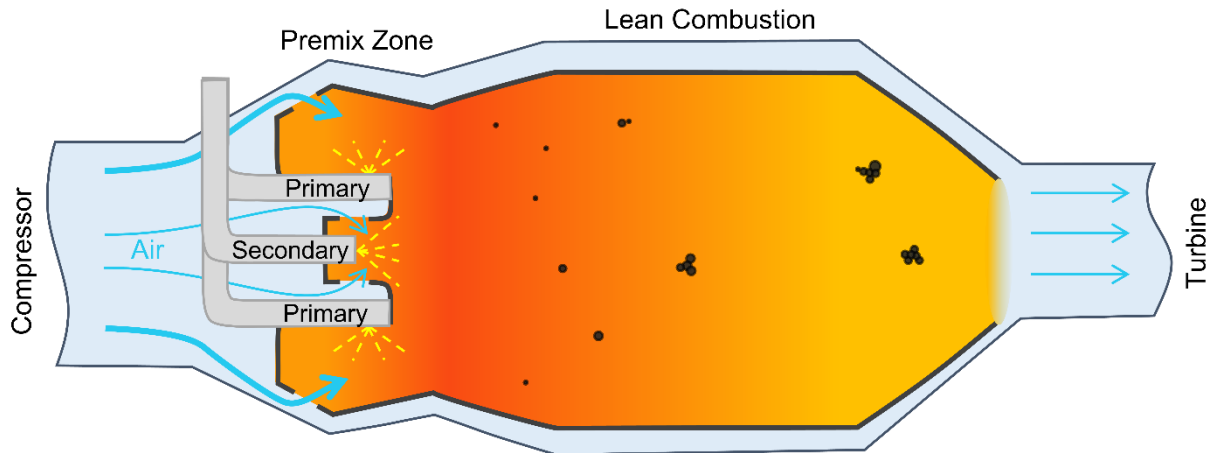


412
 413 **Figure 5: A simplified schematic of a Lean Direct Injection (LDI) combustor adapted from (Fric, 1995) which features**
 414 **a central pilot injector surrounded by multiple main injectors. These combustors usually have most or all the air flow**
 415 **into the combustor around the fuel injectors without subsequent dilution to provide intense mixing for lean combustion**
 416 **with close to premixed combustion.**

417 Lean Premixed Prevaporized (LPP) combustors aim to completely vaporize the jet fuel prior to ignition
 418 in order to have lean, premixed combustion (Figure 6). Without locally fuel-rich conditions, little to no soot will
 419 form. As with the LDI combustors, there is little dilution after the initial injection of primary air for combustion.
 420 Premixed combustion with high pressures comes with a risk of autoignition in the mixing zone so careful design
 421 of the combustor is needed to prevent such instabilities. These combustors use special fuel injectors to achieve
 422 near-premixed lean combustion conditions which tend to form significantly less soot. Both the LDI and LPP
 423 combustor designs achieve stable combustion through complex combustor design which could lead to increased
 424 cost and maintenance. So, lean conditions are favorable for emissions reduction but come with engineering
 425 challenges. Theoretically, new jet fuels with lower lean blow-off (LBO) limits could extend the lean operating
 426 range of an engine and conversely, fuels with an insufficient LBO could pose a safety risk (Undavalli et al., 2023).

427 Recently, a novel research engine called the Lean Azimuthal Flame (LEAF) combustor (not yet in
 428 commercial use) using “flameless oxidation” has been developed for soot-free and low NO_x combustion (Oliveira
 429 et al., 2021). This concept can be further improved through co-combustion of small amounts of hydrogen which
 430 extends the operating window (Miniero et al., 2023). The use of hydrogen helps to stabilize the combustion without
 431 the use of a fuel-rich pilot flame that can increase soot production as with the DAC combustors. Such concepts

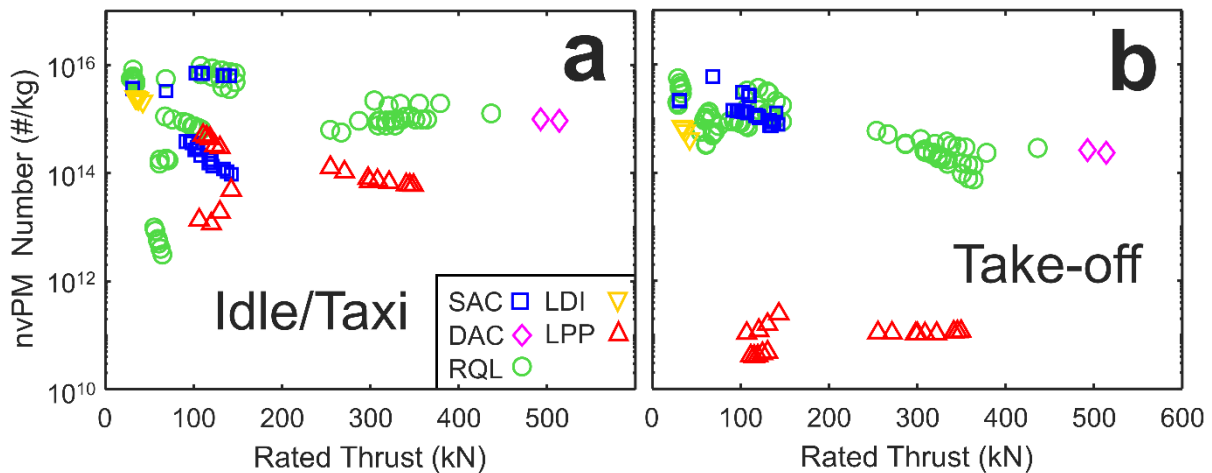
432 which require an additional fuel that cannot be used in all engines require significantly more capital to implement
 433 because additional infrastructure needs to be built to support, for example, hydrogen storage and fueling.
 434 Furthermore, such parallel infrastructure poses a safety risk if an aircraft is filled with the wrong fuel and therefore
 435 such solutions are not promoted by the (ICAO, 2018). So, combustors which achieve lean, premixed conditions
 436 are promising for achieving both low soot and low NO_x emissions but pose design challenges.



437
 438 **Figure 6: A simplified schematic of a Lean Premixed Prevaporized (LPP) combustor adapted from (Foust et al., 2012)**
 439 **which contains multiple injectors that spray fuel into the premix zone where the jet fuel completely vaporizes without**
 440 **ignition. Then, in the combustion zone the premixed fuel is ignited under fuel-lean conditions which nearly eliminate**
 441 **soot while low temperatures prevent the formation of NO_x.**

442 The ICAO provides a public database of regulated emissions with the earliest nvPM emission test dates
 443 starting in 2014 (ICAO Aircraft Engine Emissions Databank, 2023). These data are collected and reported by the
 444 engine manufacturers following the standards laid out in the ICAO Annex 16 for engine emissions certification
 445 (ICAO, 2017). Emissions are tested across the entire LTO cycle which includes idle/taxi (7% thrust), approach
 446 (30%), climb-out (80%) and take-off (100%) for both nvPM mass and number. Data submitted to the ICAO
 447 database should be collected following the procedure outlined in the ICAO Annex 16, Vol. II (ICAO, 2017).
 448 Briefly, particles are sampled at the engine exhaust with a no more than 35 m long (from probe tip to instrument
 449 inlet) heated sampling line to the measurement devices. This relatively long line, paired with the small size of
 450 aircraft soot may result in significant diffusional and thermophoretic losses due to temperature gradients as the
 451 sample cools from the exhaust temperature to sample line temperature. Since 2017, the nvPM mass and number
 452 diffusion and thermophoretic losses must be accounted for with the methods outlined in the ICAO Annex 16, Vol.
 453 II (ICAO, 2017). However, it is important to note that these losses are size-dependent, but the regulations do not
 454 require particle size measurements. Therefore, the estimate of the line loss correction may not be accurate for all
 455 engines. Figure 7 shows the nvPM number emissions normalized by the fuel flow (#/kg) at (a) idle/taxi and (b)
 456 take-off for simplicity, although approach and climb-out data are also available (ICAO Aircraft Engine Emissions
 457 Databank, 2023). Mass nvPM data shows similar trends. The main differences between nvPM mass and nvPM
 458 number are the LPP values falling closer to the other combustors with mass-based emissions compared to number
 459 based emissions. This suggests that the LPP produces fewer but larger particles than other combustors on average.
 460 Values for approach and climb-out tend to fall between those measured at the extremes for both number and mass
 461 nvPM. Combustor names are provided for all entries in the database and can be grouped by type if sufficient
 462 information is given by the manufacturer. The RQL combustors make up the majority of reported data (134 entries),
 463 followed by SAC (38), LPP (26), LDI (7) and DAC (2). Within these broad categories, there are multiple distinct
 464 implementations of these combustor types. For example, the RQL category contains the Rolls-Royce Phase5 series,
 465 Pratt & Whitney Talon series and General Electric LEC series combustors. The SAC (squares) have some of the
 466 highest emissions in the database, but a group of SAC are approximately an order of magnitude lower at idle/taxi
 467 (Fig. 7a). These lower emission SAC are modified for better performance (CFM Tech Insertion) which seems to
 468 improve emissions at low (7 and 30%) thrust with little change at high (80 and 100%) thrust. The data for RQL
 469 combustors (circles) have the most variation quite likely due to the variety of different implementations of the
 470 RQL concept compared to all other combustor types. This highlights the fact that RQL burners can have quite low
 471 particulate emissions if designed and operated properly, particularly for engines with lower static rated thrust. At
 472 take-off (Fig. 7b), the LPP combustors (triangles) clearly outperform all other combustors in the database. All of
 473 the LPP combustors are from the TAPS combustor series. At idle/taxi (Fig. 7a) LPP combustors still perform well
 474 but some RQL and modified-SAC combustors have similar or lower emissions. In an LPP combustor, all injectors
 475 are on during high thrust operation and premixed combustion can be achieved resulting in lower emissions.

476 Conversely, at low thrust only some of the injectors are used to lower the power output without creating conditions
 477 which are too lean for stable combustion which may explain the higher emissions at idle/taxi compared to take-
 478 off. A similar phenomenon has been observed in scientific studies of DAC engines where emissions were reduced
 479 significantly when both combustor stages were in use at approximately thrusts > 30% (Boies et al., 2015). The
 480 small number of entries for DAC and LDI combustors makes it difficult to draw conclusions about such
 481 combustors but the data that are provided for both fall in approximately the middle of the nvPM emission range.
 482 So, at present LPP combustors seem to perform at least as well as other combustors at idle/taxi and significantly
 483 reduce emissions at take-off resulting in the lowest overall emissions in the ICAO database. It is worth noting that
 484 engine operation can also reduce emissions, for example reduced thrust take-off has been shown to reduce fuel
 485 consumption, NO_x and black carbon (soot) emissions by 1.0–23.2%, 10.7–47.7%, and 49.0–71.7% respectively
 486 (Koudis et al., 2017).



487
 488 **Figure 7: The nvPM number as a function of an engine’s rated thrust at (a) idle/taxi (7% thrust), (b) take-off (100%).**
 489 **Combustor types represented in the database include SAC (squares), DAC (diamonds), RQL (circles), LDI (inverted**
 490 **triangles), LPP (triangles). The total nvPM number is normalized by the fuel flow (kg).**

491 While the ICAO database provides information on the mass and number of nvPM emissions, it does not
 492 include any morphological or chemical characterization of the particles. Furthermore, the data are collected by the
 493 engine manufacturers, rather than independent researchers although for a small number of engines, research
 494 measurements are also included (ICAO Aircraft Engine Emissions Databank, 2023). Thus far, the vast majority of
 495 academic studies on soot emissions from aircraft engines have been conducted on large commercial aircraft (rated
 496 thrust >26.7 kN) most with SAC combustors (Abegglen et al., 2015; Beyersdorf et al., 2014; Elser et al., 2019;
 497 Johnson et al., 2015; Liati et al., 2014; Marhaba et al., 2019; Parent et al., 2016). A few studies have explored soot
 498 from DAC (Boies et al., 2015; Johnson et al., 2015; Lobo et al., 2015b) and RQL (Brem et al., 2015; Delhaye et
 499 al., 2017; Saffaripour et al., 2017) engines. There is relatively little scientific research on soot emissions from
 500 novel aircraft engines. For example, the Water-Enhanced Turbofan (WET) concept expects to significantly reduce
 501 soot emissions during the stage where water is captured for recirculation (Kaiser et al., 2022). However, to the best
 502 of our knowledge, there are no scientific studies published on the actual measured or modeled soot emissions from
 503 WET engines. The limited number of studies characterizing soot emissions from ‘low emission’ engine technology
 504 highlights the need for more research on such engines if they will be adopted in the future. Commercial deployment
 505 of new engine technologies takes a significant amount of time and money and so, when a new technology is
 506 deployed it remains in use for many years with the life span of an average aircraft spanning from 20 – 30 years
 507 (Ceruti et al., 2019). This makes it essential to identify which technologies offer the best emissions profile before
 508 it is commercially scaled up, for example through the use of computational fluid dynamics (CFD).

509 4. Conclusions

510 Soot from aviation has a negative effect on human health and can contribute to climate change through direct
 511 radiative forcing and increasing the formation of persistent contrails. New regulations have been put into place to
 512 limit soot emissions in addition to other pollutants such as NO_x, UHC and CO. The strategies for reducing one
 513 type of pollutant may increase another with soot and NO_x emissions often at odds with one another. Non-CO₂
 514 aircraft emissions are estimated to be two thirds of aviation’s net-RF, but the uncertainties associated with the non-
 515 CO₂ terms are very high. The difficulty in reducing soot emissions from aviation comes primarily from the
 516 competing requirements which include safety, reduction of gaseous pollutants and cost. A better understanding of
 517 the role of soot and other non-CO₂ emissions is needed to properly assess trade-offs between design requirements

518 and avoid improving emissions of one pollutant while increasing another's or compromising safety. Thus, without
519 a robust understanding of the role of soot in direct and indirect radiative forcing (e.g. through contrail formation)
520 trade-offs between soot reduction and other pollutants cannot be properly accounted for.

521 Aircrafts tend to produce soot with relatively small d_m which has greater health impacts than larger soot
522 particles. Soot nucleates in locally fuel-rich zones (created by the jet fuel spray) then grows through surface growth,
523 condensation and agglomeration (Trivanovic et al., 2023). The OC/TC ratio of aircraft soot, which has implications
524 for the source apportionment (Ramadan et al., 2000), health effects (Kelly and Fussell, 2012) and optical properties
525 of soot (Kelesidis et al., 2021), depends on thrust (Elser et al., 2019; Fig. 6). Low thrust is associated with high
526 OC/TC and high with low OC/TC. Extensive oxidation reduces the number concentration and size of soot resulting
527 in smaller particles than other combustion sources (e.g. diesel). Significant progress is still needed to accurately
528 quantify this process in realistic aircraft combustors. Some progress has been made in recent years matching
529 experimental data from laboratory combustors but there are important differences between laboratory combustors
530 and real aircraft combustors and simulations are not yet able to match the output of these simplified combustors at
531 all conditions. A realistic description of BC allowed for the first time to determine conditions for synthesis of
532 carbon black (CB) with closely controlled structure and size that is crucial for its diverse applications where for
533 tire reinforcement hard agglomerates consisting of large primary particles (PP) are needed as fillers while for
534 battery electrodes such agglomerates should consist of much finer PP and for inks or paints the CB agglomerates
535 should be soft ones (Kelesidis et al., 2023a). Clearly such an understanding should be incorporated into the design
536 of aircraft engines burning fossil and/or sustainable aviation fuels as it greatly facilitates engine design and
537 operation for complete oxidation of any soot formed before its emission. The high cost and 20 – 30 year lifespan
538 of aircraft necessitates robust models to aid in combustor design and operation for further technological
539 advancements.

540 Sustainable Aviation Fuels (SAF) have the potential to significantly reduce soot emissions due to the
541 typically lower aromatic content and increased H/C ratio typically associated with these fuels in addition to
542 reductions in lifetime CO₂ emissions. Although most literature on the use of such fuels does show that it reduces
543 soot emissions, the reduction appears to be thrust dependent. So, it has the greatest effect on reducing low-thrust
544 emissions which are important for local air quality (e.g., idle) although modest reductions have also been observed
545 at high altitude cruising conditions. Several SAFs are approved for commercial use but lack of sufficient supply
546 makes it a tiny proportion of the global jet fuel supply (0.1 – 0.15% in 2022). If SAFs are blended at small
547 proportions with conventional jet fuel, the soot reduction benefits might be hardly seen. Targeted use of high SAF
548 blends on certain flights rather than low SAF blends for all flights could be the best use of a limited resource.
549 Supply issues likely will not be overcome soon, so policies mandating the use of SAF fuels should be designed in
550 a way that encourages the use of a targeted approach that will also lower soot emissions, not just life cycle CO₂.

551 Soot is primarily produced during fuel-rich combustion. So, throughout the years efforts have been made to
552 move toward fuel-lean combustion processes. The RQL combustors use a lean quenching stage after an initial rich
553 burn to ensure good combustion stability while still reducing NO_x and in some cases soot. The design of the
554 quenching stage is essential for balancing combustion efficiency, NO_x, and soot emissions from such engines. The
555 DAC combustors similarly take advantage of a pilot stage with low air to fuel ratios for combustion stability at
556 low thrust and a second main stage combustor which can be used at medium to high thrust for lean combustion
557 with a high air to fuel ratio. When both stages are in use, DAC combustors have very low soot emissions but when
558 only the pilot stage is used, soot emissions can be higher than in a traditional burner particularly at medium-low
559 thrust (e.g., ~20%). More recently, advances have been made on truly lean engine technologies. This can be
560 achieved either by using multiple injectors and high mixing rates to achieve nearly premixed combustion or
561 through mixing zones which allow for full evaporation of fuel before ignition. These lean burn engines promise
562 the lowest emissions of soot and NO_x due to the lower temperatures and lack of fuel-rich zones. High complexity
563 in such burners may result in higher maintenance costs. Finally, hydrogen can be used to help stabilize lean
564 combustion such as in the LEAF combustor which is both soot-free and low NO_x but is still under development
565 in academic laboratories. However, the ICAO is discouraging such solutions which require fuels that are not “drop-
566 in” (e.g. hydrogen), as incompatibilities between engines and fuels could pose safety risks and require significant
567 capital investment in infrastructure.

568 The combined use of fuels with low sooting propensity and operating at lean combustion conditions have
569 the potential to reduce or even eliminate soot emissions from aircraft engines. However, caution should be used
570 whenever there is a trade-off with other emissions (i.e. NO_x) as there is still significant uncertainty in the
571 contribution of soot to direct RF and its role in contrail formation. The development of computational models
572 which can accurately predict soot production from various combustor designs and modes of operation will be
573 essential for minimizing soot emissions from aircraft while balancing other considerations. This will rely on further

574 fundamental research to better understand soot nucleation rates to close the soot mass balance and match field
575 data.

576 **Competing interests**

577 The contact author has declared that none of the authors has any competing interests.

578 **Acknowledgements**

579 We gratefully acknowledge Christian Kubsch for proofreading this article. This research was funded by the Particle
580 Technology Laboratory, ETH Zurich, and in part by Swiss National Science Foundation (200020_182668,
581 250320_163243 and 206021_170729) and the Natural Sciences and Engineering Research Council of Canada
582 (NSERC CGSD3-547016-2020).

583 **References**

584 Abegglen, M., Durdina, L., Brem, B. T., Wang, J., and Rindlisbacher, T.: Effective density and mass – mobility
585 exponents of particulate matter in aircraft turbine exhaust: Dependence on engine thrust and particle size, *J*
586 *Aerosol Sci*, 88, 135–147, <https://doi.org/10.1016/j.jaerosci.2015.06.003>, 2015.

587 Agarwal, A., Speth, R. L., Fritz, T. M., Jacob, S. D., Rindlisbacher, T., Iovinelli, R., Owen, B., Miake-Lye, R. C.,
588 Sabnis, J. S., and Barrett, S. R. H.: SCOPE11 Method for Estimating Aircraft Black Carbon Mass and Particle
589 Number Emissions, *Environ Sci Technol*, 53, 1364–1373, <https://doi.org/10.1021/acs.est.8b04060>, 2019.

590 Agnolucci, P., Akgul, O., McDowall, W., and Papageorgiou, L. G.: The importance of economies of scale,
591 transport costs and demand patterns in optimising hydrogen fuelling infrastructure: An exploration with SHIPMod
592 (Spatial hydrogen infrastructure planning model), *Int J Hydrogen Energy*, 38, 11189–11201,
593 <https://doi.org/10.1016/j.ijhydene.2013.06.071>, 2013.

594 Air France KLM Sustainable Aviation Fuel:
595 https://www.afklcargo.com/CH/en/common/products_and_solutions/sustainableaviationfuel.jsp#.

596 Baldelli, A., Trivanovic, U., Sipkens, T. A., and Rogak, S. N.: On determining soot maturity: A review of the role
597 of microscopy- and spectroscopy-based techniques, *Chemosphere*, 252, 126532,
598 <https://doi.org/10.1016/j.chemosphere.2020.126532>, 2020.

599 Bendtsen, K. M., Broström, A., Koivisto, A. J., Koponen, I., Berthing, T., Bertram, N., Kling, K. I., Dal Maso, M.,
600 Kangasniemi, O., Poikkimäki, M., Loeschner, K., Clausen, P. A., Wolff, H., Jensen, K. A., Saber, A. T., and Vogel,
601 U.: Airport emission particles: Exposure characterization and toxicity following intratracheal instillation in mice,
602 *Part Fibre Toxicol*, 16, 1–23, <https://doi.org/10.1186/s12989-019-0305-5>, 2019.

603 Beyersdorf, A. J., Timko, M. T., Ziemba, L. D., Bulzan, D., Corporan, E., Herndon, S. C., Howard, R., Miake-
604 Lye, R., Thornhill, K. L., Winstead, E., Wey, C., Yu, Z., and Anderson, B. E.: Reductions in aircraft particulate
605 emissions due to the use of Fischer-Tropsch fuels, *Atmos Chem Phys*, 14, 11–23, <https://doi.org/10.5194/acp-14-11-2014>, 2014.

607 Bock, L. and Burkhardt, U.: The temporal evolution of a long-lived contrail cirrus cluster: Simulations with a
608 global climate model, *J Geophys Res*, 121, 3548–3565, <https://doi.org/10.1002/2015JD024475>, 2016.

609 Boies, A. M., Stettler, M. E. J., Swanson, J. J., Johnson, T. J., Olfert, J. S., Johnson, M., Eggersdorfer, M. L.,
610 Rindlisbacher, T., Wang, J., Thomson, K., Smallwood, G., Sevcenco, Y., Walters, D., Williams, P. I., Corbin, J.,
611 Mensah, A. A., Symonds, J., Dastanpour, R., and Rogak, S. N.: Particle emission characteristics of a gas turbine
612 with a double annular combustor, *Aerosol Science and Technology*, 49, 842–855,
613 <https://doi.org/10.1080/02786826.2015.1078452>, 2015.

614 Bond, T. C., Doherty, S. J., Fahey, D. W., Forster, P. M., Berntsen, T., DeAngelo, B. J., Flanner, M. G., Ghan, S.,
615 Kärcher, B., Koch, D., Kinne, S., Kondo, Y., Quinn, P. K., Sarofim, M. C., Schultz, M. G., Schulz, M.,
616 Venkataraman, C., Zhang, H., Zhang, S., Bellouin, N., Guttikunda, S. K., Hopke, P. K., Jacobson, M. Z., Kaiser,
617 J. W., Klimont, Z., Lohmann, U., Schwarz, J. P., Shindell, D., Storelvmo, T., Warren, S. G., and Zender, C. S.:
618 Bounding the role of black carbon in the climate system: A scientific assessment, *Journal of Geophysical Research:*
619 *Atmospheres*, 118, 5380–5552, <https://doi.org/10.1002/jgrd.50171>, 2013.

620 Bouaniche, A., Yon, J., Domingo, P., and Vervisch, L.: Analysis of the Soot Particle Size Distribution in a Laminar
621 Premixed Flame: A Hybrid Stochastic/Fixed-Sectional Approach, *Flow Turbul Combust*, 104, 753–775,
622 <https://doi.org/10.1007/s10494-019-00103-2>, 2020.

623 Brem, B. T., Durdina, L., Siegerist, F., Beyerle, P., Bruderer, K., Rindlisbacher, T., Rocci-Denis, S., Andac, M.
624 G., Zelina, J., Penanhoat, O., and Wang, J.: Effects of Fuel Aromatic Content on Nonvolatile Particulate Emissions
625 of an In-Production Aircraft Gas Turbine, *Environ Sci Technol*, 49, 13149–13157,
626 <https://doi.org/10.1021/acs.est.5b04167>, 2015.

627 Brooks, K. P., Snowden-Swan, L. J., Jones, S. B., Butcher, M. G., Lee, G. S. J., Anderson, D. M., Frye, J. G.,
628 Holladay, J. E., Owen, J., Harmon, L., Burton, F., Palou-Rivera, I., Plaza, J., Handler, R., and Shonnard, D.: Low-
629 Carbon Aviation Fuel Through the Alcohol to Jet Pathway, in: *Biofuels for Aviation: Feedstocks, Technology and*
630 *Implementation*, Elsevier Inc., 109–150, <https://doi.org/10.1016/B978-0-12-804568-8.00006-8>, 2016.

631 Camacho, J., Liu, C., Gu, C., Lin, H., Huang, Z., Tang, Q., You, X., Saggese, C., Li, Y., Jung, H., Deng, L.,
632 Wlokas, I., and Wang, H.: Mobility size and mass of nascent soot particles in a benchmark premixed ethylene
633 flame, *Combust Flame*, 162, 3810–3822, <https://doi.org/10.1016/j.combustflame.2015.07.018>, 2015.

634 Carbone, F., Gleason, K., and Gomez, A.: Soot research: Relevance and priorities by mid-century, in: *Combustion*
635 *Chemistry and the Carbon Neutral Future*, Elsevier Inc., 27–61, [https://doi.org/10.1016/B978-0-323-99213-](https://doi.org/10.1016/B978-0-323-99213-8.00007-2)
636 [8.00007-2](https://doi.org/10.1016/B978-0-323-99213-8.00007-2), 2023.

637 Cassee, F. R., Héroux, M. E., Gerlofs-Nijland, M. E., and Kelly, F. J.: Particulate matter beyond mass: Recent
638 health evidence on the role of fractions, chemical constituents and sources of emission, *Inhal Toxicol*, 25, 802–
639 812, <https://doi.org/10.3109/08958378.2013.850127>, 2013.

640 Cavalli, F., Viana, M., Yttri, K. E., Genberg, J., and Putaud, J.-P.: Toward a standardised thermal-optical protocol
641 for measuring atmospheric organic and elemental carbon: the EUSAAR protocol, *Atmos Meas Tech*, 3, 79–89,
642 <https://doi.org/10.5194/amt-3-79-2010>, 2010.

643 Ceruti, A., Marzocca, P., Liverani, A., and Bil, C.: Maintenance in aeronautics in an Industry 4.0 context: The role
644 of Augmented Reality and Additive Manufacturing, *J Comput Des Eng*, 6, 516–526,
645 <https://doi.org/10.1016/j.jcde.2019.02.001>, 2019.

646 Chong, S. T., Hassanaly, M., Koo, H., Mueller, M. E., Raman, V., and Geigle, K. P.: Large eddy simulation of
647 pressure and dilution-jet effects on soot formation in a model aircraft swirl combustor, *Combust Flame*, 192, 452–
648 472, <https://doi.org/10.1016/j.combustflame.2018.02.021>, 2018a.

649 Chong, S. T., Raman, V., Mueller, M. E., and Im, H. G.: The role of recirculation zones in soot formation in aircraft
650 combustors, *Proceedings of the ASME Turbo Expo*, 4B-2018, 1–9, <https://doi.org/10.1115/GT2018-76217>,
651 2018b.

652 Chu, H., Qi, J., Feng, S., Dong, W., Hong, R., Qiu, B., and Han, W.: Soot formation in high-pressure combustion:
653 Status and challenges, *Fuel*, 345, 128236, <https://doi.org/10.1016/j.fuel.2023.128236>, 2023.

654 Commodo, M., D’Anna, A., De Falco, G., Larciprete, R., and Minutolo, P.: Illuminating the earliest stages of the
655 soot formation by photoemission and Raman spectroscopy, *Combust Flame*, 181, 188–197,
656 <https://doi.org/10.1016/j.combustflame.2017.03.020>, 2017.

657 Commodo, M., Kaiser, K., De Falco, G., Minutolo, P., Schulz, F., D’Anna, A., and Gross, L.: On the early stages
658 of soot formation: Molecular structure elucidation by high-resolution atomic force microscopy, *Combust Flame*,
659 205, 154–164, <https://doi.org/10.1016/j.combustflame.2019.03.042>, 2019.

660 Delaval, M. N., Jonsdottir, H. R., Leni, Z., Keller, A., Brem, B. T., Siegerist, F., Schönenberger, D., Durdina, L.,
661 Elser, M., Salathe, M., Baumlin, N., Lobo, P., Burtscher, H., Liati, A., and Geiser, M.: Responses of reconstituted
662 human bronchial epithelia from normal and health-compromised donors to non-volatile particulate matter
663 emissions from an aircraft turbofan engine, *Environmental Pollution*, 307, 119521,
664 <https://doi.org/10.1016/j.envpol.2022.119521>, 2022.

665 Delhaye, D., Ouf, F. X., Ferry, D., Ortega, I. K., Penanhoat, O., Peillon, S., Salm, F., Vancassel, X., Focsa, C.,
666 Irimiea, C., Harivel, N., Perez, B., Quinton, E., Yon, J., and Gaffie, D.: The MERMOSE project: Characterization

667 of particulate matter emissions of a commercial aircraft engine, *J Aerosol Sci*, 105, 48–63,
668 <https://doi.org/10.1016/j.jaerosci.2016.11.018>, 2017.

669 Dobbins, R. A.: Soot inception temperature and the carbonization rate of precursor particles, *Combust Flame*, 130,
670 204–214, [https://doi.org/10.1016/S0010-2180\(02\)00374-7](https://doi.org/10.1016/S0010-2180(02)00374-7), 2002.

671 Durand, E., Lobo, P., Crayford, A., Sevcenco, Y., and Christie, S.: Impact of fuel hydrogen content on non-volatile
672 particulate matter emitted from an aircraft auxiliary power unit measured with standardised reference systems,
673 *Fuel*, 287, <https://doi.org/10.1016/j.fuel.2020.119637>, 2021.

674 Durdina, L., Brem, B. T., Abegglen, M., Lobo, P., Rindlisbacher, T., Thomson, K. A., Smallwood, G. J., Hagen,
675 D. E., Sierau, B., and Wang, J.: Determination of PM mass emissions from an aircraft turbine engine using particle
676 effective density, *Atmos Environ*, 99, 500–507, <https://doi.org/10.1016/j.atmosenv.2014.10.018>, 2014.

677 Durdina, L., Lobo, P., Trueblood, M. B., Black, E. A., Achterberg, S., Hagen, D. E., Brem, B. T., and Wang, J.:
678 Response of real-time black carbon mass instruments to mini-CAST soot, *Aerosol Science and Technology*, 50,
679 906–918, <https://doi.org/10.1080/02786826.2016.1204423>, 2016.

680 Durdina, L., Brem, B. T., Setyan, A., Siegerist, F., Rindlisbacher, T., and Wang, J.: Assessment of Particle
681 Pollution from Jetliners: From Smoke Visibility to Nanoparticle Counting, *Environ Sci Technol*, 51, 3534–3541,
682 <https://doi.org/10.1021/acs.est.6b05801>, 2017.

683 Durdina, L., Brem, B. T., Schönenberger, D., Siegerist, F., Anet, J. G., and Rindlisbacher, T.: Nonvolatile
684 Particulate Matter Emissions of a Business Jet Measured at Ground Level and Estimated for Cruising Altitudes,
685 *Environ Sci Technol*, 53, 12865–12872, <https://doi.org/10.1021/acs.est.9b02513>, 2019.

686 Durdina, L., Brem, B. T., Elser, M., Sch, D., Siegerist, F., and Anet, J. G.: Reduction of Nonvolatile Particulate
687 Matter Emissions of a Commercial Turbofan Engine at the Ground Level from the Use of a Sustainable Aviation
688 Fuel Blend, *Environ Sci Technol*, 55, 14576–14585, <https://doi.org/10.1021/acs.est.1c04744>, 2021.

689 Fit for 55 and ReFuelEU Aviation: <https://www.easa.europa.eu/en/light/topics/fit-55-and-refueleu-aviation>.

690 Eggersdorfer, M. L. and Pratsinis, S. E.: Agglomerates and aggregates of nanoparticles made in the gas phase,
691 *Advanced Powder Technology*, 25, 71–90, 2014.

692 Elser, M., Brem, B. T., Durdina, L., Schönenberger, D., Siegerist, F., Fischer, A., and Wang, J.: Chemical
693 composition and radiative properties of nascent particulate matter emitted by an aircraft turbofan burning
694 conventional and alternative fuels, *Atmos Chem Phys*, 19, 6809–6820, <https://doi.org/10.5194/acp-19-6809-2019>,
695 2019.

696 European Commission: Proposal for a Regulation of the European Parliament and of the council on ensuring a level
697 playing field for sustainable air transport, European Commission, 2021.

698 Foust, M. J., Thomsen, D., Stickles, R., Cooper, C., and Dodds, W.: Development of the GE aviation low emissions
699 TAPS combustor for next generation aircraft engines, 50th AIAA Aerospace Sciences Meeting Including the New
700 Horizons Forum and Aerospace Exposition, 1–9, <https://doi.org/10.2514/6.2012-936>, 2012.

701 Franzelli, B., Tardelli, L., Stöhr, M., Geigle, K. P., and Domingo, P.: Assessment of LES of intermittent soot
702 production in an aero-engine model combustor using high-speed measurements, *Proceedings of the Combustion
703 Institute*, 39, 4821–4829, <https://doi.org/10.1016/j.proci.2022.09.060>, 2023.

704 Frenklach, M.: Reaction mechanism of soot formation in flames, *Physical Chemistry Chemical Physics*, 4, 2028–
705 2037, <https://doi.org/10.1039/b110045a>, 2002.

706 Fric, T.: Low-emission combustor having perforated plate for lean direct injection, 1995.

707 Gao, K., Zhou, C. W., Meier, E. J. B., and Kanji, Z. A.: Laboratory studies of ice nucleation onto bare and internally
708 mixed soot-sulfuric acid particles, *Atmos Chem Phys*, 22, 5331–5364, <https://doi.org/10.5194/acp-22-5331-2022>,
709 2022.

710 George, R. E., Nevitt, J. S., and Verssen, J. A.: Jet aircraft operations: Impact on the air environment, *J Air Pollut
711 Control Assoc*, 22, 507–515, <https://doi.org/10.1080/00022470.1972.10469667>, 1972.

712 Gkantonas, S., Sirignano, M., Giusti, A., D'Anna, A., and Mastorakos, E.: Comprehensive soot particle size
713 distribution modelling of a model Rich-Quench-Lean burner, *Fuel*, 270, 117483,
714 <https://doi.org/10.1016/j.fuel.2020.117483>, 2020.

715 Goudeli, E., Eggersdorfer, M. L., and Pratsinis, S. E.: Coagulation-agglomeration of fractal-like particles:
716 Structure and self-preserving size distribution, *Langmuir*, 31, 1320–1327, <https://doi.org/10.1021/la504296z>,
717 2015.

718 Han, J., Elgowainy, A., Cai, H., and Wang, M. Q.: Life-cycle analysis of bio-based aviation fuels, *Bioresour*
719 *Technol*, 150, 447–456, <https://doi.org/10.1016/j.biortech.2013.07.153>, 2013.

720 Harper, J., Durand, E., Bowen, P., Pugh, D., Johnson, M., and Crayford, A.: Influence of alternative fuel properties
721 and combustor operating conditions on the nvPM and gaseous emissions produced by a small-scale RQL
722 combustor, *Fuel*, 315, 123045, <https://doi.org/10.1016/j.fuel.2021.123045>, 2022.

723 El Helou, I., Skiba, A. W., and Mastorakos, E.: Experimental Investigation of Soot Production and Oxidation in a
724 Lab-Scale Rich–Quench–Lean (RQL) Burner, *Flow Turbul Combust*, 106, 1019–1041,
725 <https://doi.org/10.1007/s10494-020-00113-5>, 2021.

726 ICAO: Annex 16 to the convention on international civil aviation: environmental protection, Vol. II - aircraft
727 engine emissions, Montreal, CA, 4th ed. pp., 2017.

728 ICAO: Sustainable Aviation Fuels Guide, 1–66 pp., 2018.

729 ICAO Aircraft Engine Emissions Databank: [https://www.easa.europa.eu/en/domains/environment/icao-aircraft-](https://www.easa.europa.eu/en/domains/environment/icao-aircraft-engine-emissions-databank)
730 [engine-emissions-databank](https://www.easa.europa.eu/en/domains/environment/icao-aircraft-engine-emissions-databank), last access: 8 August 2023.

731 Johnson, T. J., Olfert, J. S., Symonds, J. P. R., Johnson, M., Rindlisbacher, T., Swanson, J. J., Boies, A. M.,
732 Thomson, K., Smallwood, G., Walters, D., Sevcenco, Y., Crayford, A., Dastanpour, R., Rogak, S. N., Durdina, L.,
733 Bahk, Y. K., Brem, B., and Wang, J.: Effective Density and Mass-Mobility Exponent of Aircraft Turbine
734 Particulate Matter, *J Propuls Power*, 31, 573–580, <https://doi.org/10.2514/1.B35367>, 2015.

735 Kaiser, S., Schmitz, O., Ziegler, P., and Klingels, H.: The Water-Enhanced Turbofan as Enabler for Climate-
736 Neutral Aviation, *Applied Sciences*, 12, 12431, <https://doi.org/10.3390/app122312431>, 2022.

737 Kärcher, B.: Formation and radiative forcing of contrail cirrus, *Nat Commun*, 9, 1824,
738 <https://doi.org/10.1038/s41467-018-04068-0>, 2018.

739 Kelesidis, G. A. and Goudeli, E.: Self-preserving size distribution and collision frequency of flame-made
740 nanoparticles in the transition regime, *Proceedings of the Combustion Institute*, 38, 1233–1240,
741 <https://doi.org/10.1016/j.proci.2020.07.147>, 2021.

742 Kelesidis, G. A. and Pratsinis, S. E.: A perspective on gas-phase synthesis of nanomaterials: Process design, impact
743 and outlook, *Chemical Engineering Journal*, 421, 129884, <https://doi.org/10.1016/j.cej.2021.129884>, 2021.

744 Kelesidis, G. A., Goudeli, E., and Pratsinis, S. E.: Flame synthesis of functional nanostructured materials and
745 devices: Surface growth and aggregation, *Proceedings of the Combustion Institute*, 36, 29–50,
746 <https://doi.org/10.1016/j.proci.2016.08.078>, 2017a.

747 Kelesidis, G. A., Goudeli, E., and Pratsinis, S. E.: Morphology and mobility diameter of carbonaceous aerosols
748 during agglomeration and surface growth, *Carbon*, 121, 527–535, <https://doi.org/10.1016/j.carbon.2017.06.004>,
749 2017b.

750 Kelesidis, G. A., Kholghy, M. R., Zuercher, J., Robertz, J., Allemann, M., Duric, A., and Pratsinis, S. E.: Light
751 scattering from nanoparticle agglomerates, *Powder Technol*, 365, 52–59,
752 <https://doi.org/10.1016/j.powtec.2019.02.003>, 2020.

753 Kelesidis, G. A., Bruun, C. A., and Pratsinis, S. E.: The impact of organic carbon on soot light absorption, *Carbon*,
754 172, 742–749, <https://doi.org/10.1016/j.carbon.2020.10.032>, 2021.

755 Kelesidis, G. A., Neubauer, D., Fan, L. S., Lohmann, U., and Pratsinis, S. E.: Enhanced Light Absorption and
756 Radiative Forcing by Black Carbon Agglomerates, *Environ Sci Technol*, 56, 8610–8618,
757 <https://doi.org/10.1021/acs.est.2c00428>, 2022.

758 Kelesidis, G. A., Benz, S., and Pratsinis, S. E.: Process design for carbon black size and morphology, *Carbon*, 213,
759 118255, <https://doi.org/10.1016/j.carbon.2023.118255>, 2023a.

760 Kelesidis, G. A., Nagarkar, A., Trivanovic, U., and Pratsinis, S. E.: Toward Elimination of Soot Emissions from
761 Jet Fuel Combustion, *Environ Sci Technol*, 57, 10276–10283, <https://doi.org/10.1021/acs.est.3c01048>, 2023b.

762 Kelly, F. J. and Fussell, J. C.: Size, source and chemical composition as determinants of toxicity attributable to
763 ambient particulate matter, <https://doi.org/10.1016/j.atmosenv.2012.06.039>, December 2012.

764 Khalid, S. A., Wojno, J. P., Breeze-Stringfellow, A., Lurie, D. P., Wood, T. H., Ramakrishnan, K., and Paliath,
765 U.: Open rotor designs for low noise and high efficiency, Proceedings of the ASME Turbo Expo, GT2013-94736,
766 <https://doi.org/10.1115/GT2013-94736>, 2013.

767 Kholghy, M., Saffaripour, M., Yip, C., and Thomson, M. J.: The evolution of soot morphology in a laminar coflow
768 diffusion flame of a surrogate for Jet A-1, *Combust Flame*, 160, 2119–2130,
769 <https://doi.org/10.1016/j.combustflame.2013.04.008>, 2013.

770 Kim, D., Ekoto, I., Colban, W. F., and Miles, P. C.: In-cylinder CO and UHC imaging in a light-duty diesel engine
771 during PPCI low-temperature combustion, *SAE Int J Fuels Lubr*, 1, 933–956, <https://doi.org/10.4271/2008-01-1602>, 2009.

773 Koudis, G. S., Hu, S. J., Majumdar, A., Jones, R., and Stettler, M. E. J.: Airport emissions reductions from reduced
774 thrust takeoff operations, *Transp Res D Transp Environ*, 52, 15–28, <https://doi.org/10.1016/j.trd.2017.02.004>,
775 2017.

776 Lee, D. S., Fahey, D. W., Skowron, A., Allen, M. R., Burkhardt, U., Chen, Q., Doherty, S. J., Freeman, S., Forster,
777 P. M., Fuglestedt, J., Gettelman, A., De León, R. R., Lim, L. L., Lund, M. T., Millar, R. J., Owen, B., Penner, J.
778 E., Pitari, G., Prather, M. J., Sausen, R., and Wilcox, L. J.: The contribution of global aviation to anthropogenic
779 climate forcing for 2000 to 2018, *Atmos Environ*, 244, <https://doi.org/10.1016/j.atmosenv.2020.117834>, 2021.

780 Liati, A., Brem, B. T., Durdina, L., Vöggtli, M., Dasilva, Y. A. R., Eggenschwiler, P. D., and Wang, J.: Electron
781 microscopic study of soot particulate matter emissions from aircraft turbine engines, *Environ Sci Technol*, 48,
782 10975–10983, <https://doi.org/10.1021/es501809b>, 2014.

783 Liati, A., Schreiber, D., Alpert, P. A., Liao, Y., Brem, B. T., Corral Arroyo, P., Hu, J., Jonsdottir, H. R., Ammann,
784 M., and Dimopoulos Eggenschwiler, P.: Aircraft soot from conventional fuels and biofuels during ground idle and
785 climb-out conditions: Electron microscopy and X-ray micro-spectroscopy, *Environmental Pollution*, 247, 658–
786 667, <https://doi.org/10.1016/j.envpol.2019.01.078>, 2019.

787 Liu, Y., Sun, X., Sethi, V., Nalianda, D., Li, Y. G., and Wang, L.: Review of modern low emissions combustion
788 technologies for aero gas turbine engines, *Progress in Aerospace Sciences*, 94, 12–45,
789 <https://doi.org/10.1016/j.paerosci.2017.08.001>, 2017.

790 Lobo, P., Christie, S., Khandelwal, B., Blakey, S. G., and Raper, D. W.: Evaluation of Non-volatile Particulate
791 Matter Emission Characteristics of an Aircraft Auxiliary Power Unit with Varying Alternative Jet Fuel Blend
792 Ratios, *Energy and Fuels*, 29, 7705–7711, <https://doi.org/10.1021/acs.energyfuels.5b01758>, 2015a.

793 Lobo, P., Durdina, L., Smallwood, G. J., Rindlisbacher, T., Siegerist, F., Black, E. A., Yu, Z., Mensah, A. A.,
794 Hagen, D. E., Miake-Lye, R. C., Thomson, K. A., Brem, B. T., Corbin, J. C., Abegglen, M., Sierau, B., Whitefield,
795 P. D., and Wang, J.: Measurement of aircraft engine non-volatile PM emissions: Results of the Aviation-Particle
796 Regulatory Instrumentation Demonstration Experiment (A-PRIDE) 4 campaign, *Aerosol Science and Technology*,
797 49, 472–484, <https://doi.org/10.1080/02786826.2015.1047012>, 2015b.

798 Marcolli, C., Mahrt, F., and Kärcher, B.: Soot PCF: Pore condensation and freezing framework for soot aggregates,
799 *Atmos Chem Phys*, 21, 7791–7843, <https://doi.org/10.5194/acp-21-7791-2021>, 2021.

800 Marhaba, I., Ferry, D., Laffon, C., Regier, T. Z., Ouf, F., and Parent, P.: Aircraft and MiniCAST soot at the
801 nanoscale, *Combust Flame*, 204, 278–289, <https://doi.org/10.1016/j.combustflame.2019.03.018>, 2019.

802 Märkl, R. S., Voigt, C., Sauer, D., Dischl, R. K., Kaufmann, S., Harlaß, T., Hahn, V., Roiger, A., Weiß-Rehm, C.,
803 Burkhardt, U., Schumann, U., Marsing, A., Scheibe, M., Dörnbrack, A., Renard, C., Gauthier, M., Swann, P.,
804 Madden, P., Luff, D., Sallinen, R., Schripp, T., and Le Clercq, P.: Powering aircraft with 100% sustainable aviation

805 fuel reduces ice crystals in contrails, *Atmos Chem Phys*, 24, 3813–3837, [https://doi.org/10.5194/acp-24-3813-](https://doi.org/10.5194/acp-24-3813-2024)
806 2024, 2024.

807 Masiol, M. and Harrison, R. M.: Aircraft engine exhaust emissions and other airport-related contributions to
808 ambient air pollution: A review, *Atmos Environ*, 95, 409–455, <https://doi.org/10.1016/j.atmosenv.2014.05.070>,
809 2014.

810 Messerer, A., Niessner, R., and Pöschl, U.: Comprehensive kinetic characterization of the oxidation and
811 gasification of model and real diesel soot by nitrogen oxides and oxygen under engine exhaust conditions:
812 Measurement, Langmuir-Hinshelwood, and Arrhenius parameters, *Carbon*, 44, 307–324,
813 <https://doi.org/10.1016/j.carbon.2005.07.017>, 2006.

814 Miniero, L., Pandey, K., De Falco, G., D’Anna, A., and Noiray, N.: Soot-free and low-NO combustion of Jet A-1
815 in a lean azimuthal flame (LEAF) combustor with hydrogen injection, *Proceedings of the Combustion Institute*,
816 39, 4309–4318, <https://doi.org/10.1016/j.proci.2022.08.006>, 2023.

817 Mongia, H. C.: GE aviation low emissions combustion technology evolution, *SAE Technical Papers*, 776–790,
818 <https://doi.org/10.4271/2007-01-3924>, 2007.

819 Montzka, S. A., Dlugokencky, E. J., and Butler, J. H.: Non-CO₂ greenhouse gases and climate change, *Nature*,
820 476, 43–50, <https://doi.org/10.1038/nature10322>, 2011.

821 Moore, R. H., Thornhill, K. L., Weinzierl, B., Sauer, D., D’Ascoli, E., Kim, J., Lichtenstern, M., Scheibe, M.,
822 Beaton, B., Beyersdorf, A. J., Barrick, J., Bulzan, D., Corr, C. A., Crosbie, E., Jurkat, T., Martin, R., Riddick, D.,
823 Shook, M., Slover, G., Voigt, C., White, R., Winstead, E., Yasky, R., Ziemba, L. D., Brown, A., Schlager, H., and
824 Anderson, B. E.: Biofuel blending reduces particle emissions from aircraft engines at cruise conditions, *Nature*,
825 543, 411–415, <https://doi.org/10.1038/nature21420>, 2017.

826 National Academies of Sciences Engineering and Medicine: Options for Reducing Lead Emissions from Piston-
827 Engine Aircraft, <https://doi.org/10.17226/26050>, 2021.

828 Nguyen, T. H., Tri Nguyen, P., and Garnier, F.: Evaluation of the relationship between the aerothermodynamic
829 process and operational parameters in the high-pressure turbine of an aircraft engine, *Aerosp Sci Technol*, 86, 93–
830 105, <https://doi.org/10.1016/j.ast.2019.01.011>, 2019.

831 Niranjana, R. and Thakur, A. K.: The toxicological mechanisms of environmental soot (black carbon) and carbon
832 black: Focus on Oxidative stress and inflammatory pathways, *Front Immunol*, 8, 763,
833 <https://doi.org/10.3389/fimmu.2017.00763>, 2017.

834 Novic, A. S., Troth, D. L. L., Notardonato, J., Novick, A. S., Troth, D. L. L., and Notardonato, J.: Multifuel
835 Evaluation of Rich/Quench/Lean Combustor, in: *Proceedings of the ASME 1983 International Gas Turbine*
836 *Conference and Exhibit*, 1–8, <https://doi.org/10.1115/83-GT-140>, 1983.

837 Oliveira, P. M. De, Fredrich, D., Falco, G. De, Helou, I. El, Anna, A. D., Giusti, A., and Mastorakos, E.: Soot-
838 Free Low-NO_x Aeronautical Combustor Concept: The Lean Azimuthal Flame for Kerosene Sprays, *Energy and*
839 *Fuels*, 35, 7092–7106, <https://doi.org/10.1021/acs.energyfuels.0c03860>, 2021.

840 Parent, P., Laffon, C., Marhaba, I., Ferry, D., Regier, T. Z., Ortega, I. K., Chazallon, B., Carpentier, Y., and Focsa,
841 C.: Nanoscale characterization of aircraft soot: A high-resolution transmission electron microscopy, Raman
842 spectroscopy, X-ray photoelectron and near-edge X-ray absorption spectroscopy study, *Carbon*, 101, 86–100,
843 <https://doi.org/10.1016/j.carbon.2016.01.040>, 2016.

844 Prabhakar, N., Heyerdahl, L., Jha, A., and Karbowski, D.: Energy Impacts of Electric Aircraft: An Overview,
845 *AIAA AVIATION 2022 Forum*, <https://doi.org/10.2514/6.2022-4119>, 2022.

846 Ramadan, Z., Song, X. H., and Hopke, P. K.: Identification of sources of phoenix aerosol by positive matrix
847 factorization, *J Air Waste Manage Assoc*, 50, 1308–1320, <https://doi.org/10.1080/10473289.2000.10464173>,
848 2000.

849 Rissler, J., Swietlicki, E., Bengtsson, A., Boman, C., Pagels, J., Sandström, T., Blomberg, A., and Löndahl, J.:
850 Experimental determination of deposition of diesel exhaust particles in the human respiratory tract, *J Aerosol Sci*,
851 48, 18–33, <https://doi.org/10.1016/j.jaerosci.2012.01.005>, 2012.

852 Rizk, N. K. and Mongia, H. C.: Ultra-Low NO_x Rich-Lean Combustion, American Society of Mechanical
853 Engineers, 1990.

854 Saffaripour, M., Tay, L. L., Thomson, K. A., Smallwood, G. J., Brem, B. T., Durdina, L., and Johnson, M.: Raman
855 spectroscopy and TEM characterization of solid particulate matter emitted from soot generators and aircraft turbine
856 engines, *Aerosol Science and Technology*, 51, 518–531, <https://doi.org/10.1080/02786826.2016.1274368>, 2017.

857 Schäfer, A. W., Barrett, S. R. H., Doyme, K., Dray, L. M., Gnadt, A. R., Self, R., O’Sullivan, A., Synodinos, A.
858 P., and Torija, A. J.: Technological, economic and environmental prospects of all-electric aircraft, *Nat Energy*, 4,
859 160–166, <https://doi.org/10.1038/s41560-018-0294-x>, 2019.

860 Schäppi, R., Rutz, D., Dähler, F., Muroyama, A., Haueter, P., Lilliestam, J., Patt, A., Furler, P., and Steinfeld, A.:
861 Drop-in fuels from sunlight and air, *Nature*, 601, 63–68, <https://doi.org/10.1038/s41586-021-04174-y>, 2022.

862 Schripp, T., Herrmann, F., Oßwald, P., Köhler, M., Zschocke, A., Weigelt, D., Mroch, M., and Werner-Spatz, C.:
863 Particle emissions of two unblended alternative jet fuels in a full scale jet engine, *Fuel*, 256,
864 <https://doi.org/10.1016/j.fuel.2019.115903>, 2019.

865 Schripp, T., Grein, T., Zinsmeister, J., Oßwald, P., Köhler, M., Müller-Langer, F., Hauschild, S., Marquardt, C.,
866 Scheuermann, S., Zschocke, A., and Posselt, D.: Technical application of a ternary alternative jet fuel blend –
867 Chemical characterization and impact on jet engine particle emission, *Fuel*, 288,
868 <https://doi.org/10.1016/j.fuel.2020.119606>, 2021.

869 Schulz, F., Commodo, M., Kaiser, K., De Falco, G., Minutolo, P., Meyer, G., D’Anna, A., and Gross, L.: Insights
870 into incipient soot formation by atomic force microscopy, *Proceedings of the Combustion Institute*, 37, 885–892,
871 <https://doi.org/10.1016/j.proci.2018.06.100>, 2019.

872 Sharma, A., Mukut, K. M., Roy, S. P., and Goudeli, E.: The coalescence of incipient soot clusters, *Carbon*, 180,
873 215–225, <https://doi.org/10.1016/j.carbon.2021.04.065>, 2021.

874 Staples, M. D., Malina, R., Suresh, P., Hileman, J. I., and Barrett, S. R. H.: Aviation CO₂emissions reductions
875 from the use of alternative jet fuels, *Energy Policy*, 114, 342–354, <https://doi.org/10.1016/j.enpol.2017.12.007>,
876 2018.

877 Stettler, M. E. J., Boies, A. M., Petzold, A., and Barrett, S. R. H.: Global civil aviation black carbon emissions,
878 *Environ Sci Technol*, 47, 10397–10404, <https://doi.org/10.1021/es401356v>, 2013.

879 Stuber, N., Forster, P., Rädcl, G., and Shine, K.: The importance of the diurnal and annual cycle of air traffic for
880 contrail radiative forcing, *Nature*, 441, 864–867, <https://doi.org/10.1038/nature04877>, 2006.

881 Teoh, R., Schumann, U., Majumdar, A., and Stettler, M. E. J.: Mitigating the Climate Forcing of Aircraft Contrails
882 by Small-Scale Diversions and Technology Adoption, *Environ Sci Technol*, 54, 2941–2950,
883 <https://doi.org/10.1021/acs.est.9b05608>, 2020.

884 Teoh, R., Schumann, U., Gryspeerdt, E., Shapiro, M., Molloy, J., Koudis, G., Voigt, C., and Stettler, M. E. J.:
885 Aviation contrail climate effects in the North Atlantic from 2016 to 2021, *Atmos Chem Phys*, 22, 10919–10935,
886 <https://doi.org/10.5194/acp-22-10919-2022>, 2022a.

887 Teoh, R., Schumann, U., Voigt, C., Schripp, T., Shapiro, M., Engberg, Z., Molloy, J., Koudis, G., and Stettler, M.
888 E. J.: Targeted Use of Sustainable Aviation Fuel to Maximize Climate Benefits, *Environ Sci Technol*, 56, 17246–
889 17255, <https://doi.org/10.1021/acs.est.2c05781>, 2022b.

890 Teoh, R., Engberg, Z., Shapiro, M., Dray, L., and Stettler, M. E. J.: The high-resolution Global Aviation emissions
891 Inventory based on ADS-B (GAIA) for 2019–2021, *Atmos Chem Phys*, 24, 725–744, [https://doi.org/10.5194/acp-
892 24-725-2024](https://doi.org/10.5194/acp-24-725-2024), 2024.

893 Testa, B., Durdina, L., Alpert, P. A., Mahrt, F., Dreimol, C. H., Edebeli, J., Spirig, C., Decker, Z. C. J., Anet, J.,
894 and Kanji, Z. A.: Soot aerosols from commercial aviation engines are poor ice-nucleating particles at cirrus cloud
895 temperatures, *Atmos Chem Phys*, 24, 4537–4567, <https://doi.org/10.5194/acp-24-4537-2024>, 2024.

896 Trivanovic, U., Kelesidis, G. A., and Pratsinis, S. E.: High-throughput generation of aircraft-like soot, *Aerosol
897 Science and Technology*, 56, 732–743, <https://doi.org/10.1080/02786826.2022.2070055>, 2022.

898 Trivanovic, U., Pereira Martins, M., Benz, S., Kelesidis, G. A., and Pratsinis, S. E.: Dynamics of soot surface
899 growth and agglomeration by enclosed spray combustion of jet fuel, *Fuel*, 342, 127864, 2023.

900 Undavalli, V., Gbadamosi Olatunde, O. B., Boylu, R., Wei, C., Haeker, J., Hamilton, J., and Khandelwal, B.:
901 Recent advancements in sustainable aviation fuels, *Progress in Aerospace Sciences*, 136, 100876,
902 <https://doi.org/10.1016/j.paerosci.2022.100876>, 2023.

903 Vander Wal, R. L., Bryg, V. M., and Hays, M. D.: Fingerprinting soot (towards source identification): Physical
904 structure and chemical composition, *J Aerosol Sci*, 41, 108–117, <https://doi.org/10.1016/j.jaerosci.2009.08.008>,
905 2010.

906 Vander Wal, R. L., Bryg, V. M., and Huang, C. H.: Aircraft engine particulate matter: Macro- micro- and
907 nanostructure by HRTEM and chemistry by XPS, *Combust Flame*, 161, 602–611,
908 <https://doi.org/10.1016/j.combustflame.2013.09.003>, 2014.

909 Wang, H.: Formation of nascent soot and other condensed-phase materials in flames, *Proceedings of the*
910 *Combustion Institute*, 33, 41–67, <https://doi.org/10.1016/j.proci.2010.09.009>, 2011.

911 Xue, X., Hui, X., Vannorsdall, P., Singh, P., and Sung, C. J.: The blending effect on the sooting tendencies of
912 alternative/conventional jet fuel blends in non-premixed flames, *Fuel*, 237, 648–657,
913 <https://doi.org/10.1016/j.fuel.2018.09.157>, 2019.

914 Yang, Y., Boehman, A. L., and Santoro, R. J.: A study of jet fuel sooting tendency using the threshold sooting
915 index (TSI) model, *Combust Flame*, 149, 191–205, <https://doi.org/10.1016/j.combustflame.2006.11.007>, 2007.

916